The Biological Effects of HIV-1 Nef on the Development of B-cell Lymphoma

By

Riyaadh Ahmed

AHMRIY003

SUBMITTED TO THE UNIVERSITY OF CAPE TOWN

In fulfilment of the requirements for the degree:

MSc(Med) in Haematology

Faculty of Health Sciences

UNIVERSITY OF CAPE TOWN

January 2022

Supervisor: A/Prof Shaheen Mowla

Division of Haematology, Department of Pathology, Faculty of Health Sciences,

University of Cape Town.

Declaration

I, ……**Riyaadh Ahmed**……, hereby declare that the work on which this dissertation/thesis is based is my original work (except where acknowledgements indicate otherwise) and that neither the whole work nor any part of it has been, is being, or is to be submitted for another degree in this or any other university.

I empower the university to reproduce for the purpose of research either the whole or any portion of the contents in any manner whatsoever.

Signature: Signed by candidate

Date: ……..…20 January 2022…….

Acknowledgements

First and foremost, I praise and thank Allah (SWT) for granting me the strength and patience to complete my Master's degree and write my thesis, especially on those days when I wanted to give up.

Nothing in my life would be accomplished without the support of my family. To my mother and step-father, thank you for all the prayers, support and encouragement that you gave me throughout my university career. To my older brother, for all the support and for always showing a genuine interest in my research topic, despite not being familiar with biomedical research.

Navigating through my lab work and writing up my dissertation was no easy feat. However, it would not have been possible without the support of the students and staff of the Division of Haematology. To my fellow lab mates: Leo, Lungile, Aaliyah, Beatrice and Zahra, thank you for all the kindness, jokes and daily conversations. Thank you all for always going out of your way to help me with whatever lab issue I was facing. A massive thank you to the division of Haematology staff members. To Jean, our unofficial lab godmother/aunty, thank you for everything that you do, for always fighting for and supporting us students and allowing our lab to run smoothly. I will always appreciate the warmth and generosity you have shown me as well as all the interesting and funny conversations we have every week. To Cylene and Coleen, thank you for all the interesting conversations, especially during our lunch breaks in the Tea room. To Associate Professors Jessica Oppie and Karen Shires, for the kindness they have shown me. My deepest gratitude to Dr Glenda Davidson, for continuously assisting me in performing compensation on my flow cytometry data.

To my friend and fellow scientist, Malika Gabier, thank you for all the conversations we had during our breaks, whether it was lab-related or just about life in general, and for inspiring me to be a better scientist.

A special thank you to the Prince Lab especially Dr Supratim Biswas and Saif Khan for their assistance.

I would also like to sincerely thank the National Research Foundation (NRF) for financially supporting me throughout my Master's degree.

Finally, I would like to thank my research supervisor, Associate Professor Shaheen Mowla. I can't even begin to describe how eternally grateful I am to have you as my supervisor these past few years. The door to your office was always open whenever I ran into an issue or had a question about my lab work or writing. Thank you for continuously being patient with me and guiding me throughout this journey with your expertise and overall positivity, allowing me to flourish as a scientist.

Table of Contents

List of Figures

Chapter 1

Chapter 2

Chapter 3

List of Tables

Chapter 2

Chapter 3

Abbreviations

7-AAD	7-Amino-actinomycin
AID/AICDA	Activation Induced Cytidine Deaminase
AKT	Protein Kinase B
ANOVA	Analysis of Variance
AP-1	Activator Protein-1
AP-2	Activator Protein-2
ARRP-Nef	AIDS Research and Reference Reagent Program Nef Protein
ART	Anti-Retroviral Treatment
ATCC	American Type Culture Collection
BCA	Bicinchoninic acid
BCL-2	B-cell Lymphoma 2
BCL-6	B-cell Lymphoma 6
Bcl-xL	B-cell Lymphoma-extra large
BL	Burkitt Lymphoma
BrdU	Bromodeoxyuridine
BSA	Bovine Serum Albumin
CAM Model	Chorioallantoic membrane Model
CDKs	Cyclin-Dependent Kinases
CE	Cytoplasmic Extract
CNE	Chromatin-bound Nuclear Extract
CSKE	Cytoskeletal Extract
CXCR1	C-X-C Motif Chemokine Receptor 1
CXCR2	C-X-C Motif Chemokine Receptor 2
DLBCL	Diffuse Large B-cell Lymphoma

DMEM	Dulbecco's Modified Eagle Medium
DMSO	Dimethyl sulfoxide
DNA	Deoxyribonucleic acid
DSBs	Double-Stranded Breaks
DTT	Dithiothreitol
DZ	Dark Zone
EBV	Epstein-Barr Virus
ECL	Enhanced chemiluminescence
EDTA	Ethylenediaminetetraacetic acid
ERK	Extracellular Signal-Regulated Kinase
FBS	Fetal Bovine Serum
g	Gravity
GC	Germinal Centre
Hck	Hematopoietic cell kinase
HIV	Human Immunodeficiency Virus
HIV-BL	HIV-associated Burkitt Lymphoma
HRP	Horseradish Peroxidase
IG	Immunoglobulin
IGH	Immunoglobulin Heavy Chain
KS	Kaposi's Sarcoma
KSHV	Kaposi's Sarcoma-associated Herpes Virus
LCL	Lymphoblastoid cells
LMP-1	Latent Membrane Protein-1
lncRNA	long noncoding RNA
MAPK	Mitogen-activated protein kinase
ME	Membrane Extract
MHC-I	Major Histocompatibility Complex Class I

mTOR	mammalian target of rapamycin
MYC	V-myc avian myelocytomatosis viral oncogene homolog
NE	Nuclear Extract
Nef	Negative Factor
NHL	Non-Hodgkin Lymphoma
NIH	National Institute of Health
NIH ARRP	NIH AIDS Research and Reference Reagent Program
NSCLC	Non-Small Cell Lung Cancer
P/S	Penicillin/Streptomycin
PAK	p21 (RAC1) Activated Kinase
PAX 5	Paired Box 5
PBL	Plasmablastic Lymphoma
PBS	Phosphate-buffered Saline
PE-Annexin V	Phycoerythrin-Annexin V
pET-14b-Nef SF2	Recombinant HIS-tagged HIV-1 Nef protein
PI	Propidium Iodide
PI3K	Phosphoinositide 3-kinases
pRB	Retinoblastoma protein
PTEN	Phosphatase and tensin homolog
RNA	Ribonucleic acid
RIPA	Radio-Immunoprecipitation Assay
RPM	Revolutions per minute
RPMI	Roswell Park Memorial Institute
RT	Room Temperature
SDS-PAGE	Sodium Dodecyl Sulphate-Polyacrylamide Gel Electrophoresis
SMH	Somatic Hypermutation
Src	Proto-oncogene tyrosine-protein kinase Src (Sarcoma)

STAT3	Signal Transducer and Activator of Transcription 3
Tat	Trans-activator of Transcription
TCR	T-cell Receptor
USA	United States of America
vIL-6	Viral Interleukin-6
WHO	World Health Organization

Abstract

The incidence of HIV-associated cancers is significantly higher within the South African population compared to elsewhere in the world due to South Africa having one of the highest HIV burdens compared to the rest of the world. Burkitt lymphoma (BL) is an extremely aggressive cancer that is considered to be a highly prevalent subtype of Non-Hodgkin Lymphoma (NHL) affiliated with chronic HIV infection. While the immunosuppressive aspect of HIV remains a primary cause for the increased occurrence of cancer amongst HIV positive patients, new research demonstrates that the virus can have direct oncogenic effects, often through the action of specific virally-encoded proteins. The latter can act alone or collaboratively with cellular proteins, as well as with oncoproteins of established oncogenic viruses such as the Kaposi's Sarcoma-associated Herpes Virus (KSHV), or with Epstein-Barr Virus (EBV). To date, convincing evidence assign oncogenic activity to the HIV viral proteins Trans-activator of Transcription (Tat) and p17 in the progression of B-cell lymphomagenesis. Of particular interest to this study is the HIV-1 viral protein Nef (Negative Factor) which has been reported to have an oncogenic role in several cancer types including Kaposi's Sarcoma (KS) and Non-Small Cell Lung Cancer (NSCLC). However, the role of HIV-1 Nef in B-cell lymphoma, including BL, remains largely unexplored. Previous work performed in our research laboratory demonstrated that HIV-1 Nef protein could enhance the expression of two key lymphoma promoting factors, c-MYC and Activation Induced Cytidine Deaminase (AID), in BL cells and promoted genomic instability. The current study aimed to further explore the oncogenic effects of HIV-1 protein Nef in the development of BL. Furthermore, the potential internalization of recombinant Nef protein by B-cells during extracellular exposure was examined. Herein, we utilized cellular-based assays to examine alterations in the proliferation, the cell cycle and apoptosis of BL cells that have been extracellularly exposed to recombinant Nef protein. Our findings reveal that the proliferation of BL cells was enhanced in response

to Nef exposure. Furthermore, the expression of the cyclin proteins A, B1 and E2 were found to be increased in Nef-exposed BL cells, which could account for the enhanced proliferation. No major changes in the cell cycle profile of BL cells were noted upon exposure to Nef. While a sub-G1 peak was noted during cell cycle analysis, Annexin V/7-Amino-actinomycin (7-AAD) staining confirmed that this observation was an anomaly, confirming that the Nef protein did not enhance apoptosis in BL cells. Additionally, the Nef protein did not provide any protective effect against apoptosis in BL cells exposed to the chemotherapeutic agent Doxorubicin. Finally, investigation of the potential internalization of the Nef protein by B-cells indicated that Nef may be trafficked to both the cytoplasm and the nucleus. However, this remains inconclusive due to Nef being detected in negative control samples. Overall, this study generated novel data on the oncogenic role of HIV-1 protein Nef in the development of BL, demonstrating that this viral protein has the ability to enhance proliferation of BL cells. Additionally, Nef was shown to alter the expression of cellular cyclin proteins, which could be one of the mechanisms via which proliferation is enhanced. This data allows for a better understanding of the oncogenic role of Nef in the development of B-cell lymphoma, and contributes to our observation of enhanced disease severity and progression in HIV infected people who develop BL. Future studies will focus on further defining the oncogenic potential of Nef in aggressive B-cell lymphomas by examining its effect on other oncogenic processes/pathways which define hallmarks of cancer, including cell migration and invasion, autophagy and angiogenesis, as well as its effect on oncogenic signalling pathways. In addition to this, further optimization of the experimental design used to assess the potential internalization of the Nef protein by BL-cells is recommended for future work. Ultimately, more research must be undertaken to further elucidate the oncogenic role of HIV-1 Nef protein in HIV-associated lymphomas such as BL.

Chapter 1

Introduction

1.1 HIV-associated Cancers in sub-Saharan Africa

Cancer can be described as a group of diseases that involve unregulated proliferation of abnormal cells, which can cause the emergence of malignant tumours. Globally in 2020, 19.3 million new cases of cancer were estimated to have arisen with almost 10 million cancer-related deaths. Due to risk factors, such as population growth and age, the incidence of cancer is gradually increasing in Africa with a higher incidence of cancer cases expected by 2030 due to a projected growth of 50% in the African population (resulting in an estimated total of 1.52 billion people) [1-4]. Many sub-Saharan African (SSA) countries report prostate, breast and cervical cancer to be the most prevalent cancers within the population, with the number of cancer cases expected to increase two-fold over the next 20 years [5].

In addition to the existing burden of cancer, the SSA region holds the highest HIV prevalence worldwide, and South Africa in particular has one of the highest HIV burdens in the world, with an estimated 8,2 million South Africans living with the virus (prevalence rate of 13,7%) in 2021 [6, 8]. Consequently, the incidence of specific cancers that are associated with HIV infection (HIV-associated cancers) is significantly higher within the South African population when compared to elsewhere in the world [8-10]. Of particular interest to this study is HIV-associated Burkitt lymphoma, a subtype of Non-Hodgkin Lymphoma (NHL), the latter being reported among the top 10 cancers affecting the South African population in 2020 [2].

1.2 HIV-associated Non-Hodgkin Lymphoma

NHL can be defined as a group of haematological cancers that originate from aberrant B-lymphocytes (B-cells); T-lymphocytes (T-cells) and Natural Killer (NK) cells. NHL can be further split into several clinical variants that deviate

from each other based on specific genetic markers and their molecular structure [18, 19]. An analysis of bone marrow biopsies collected between

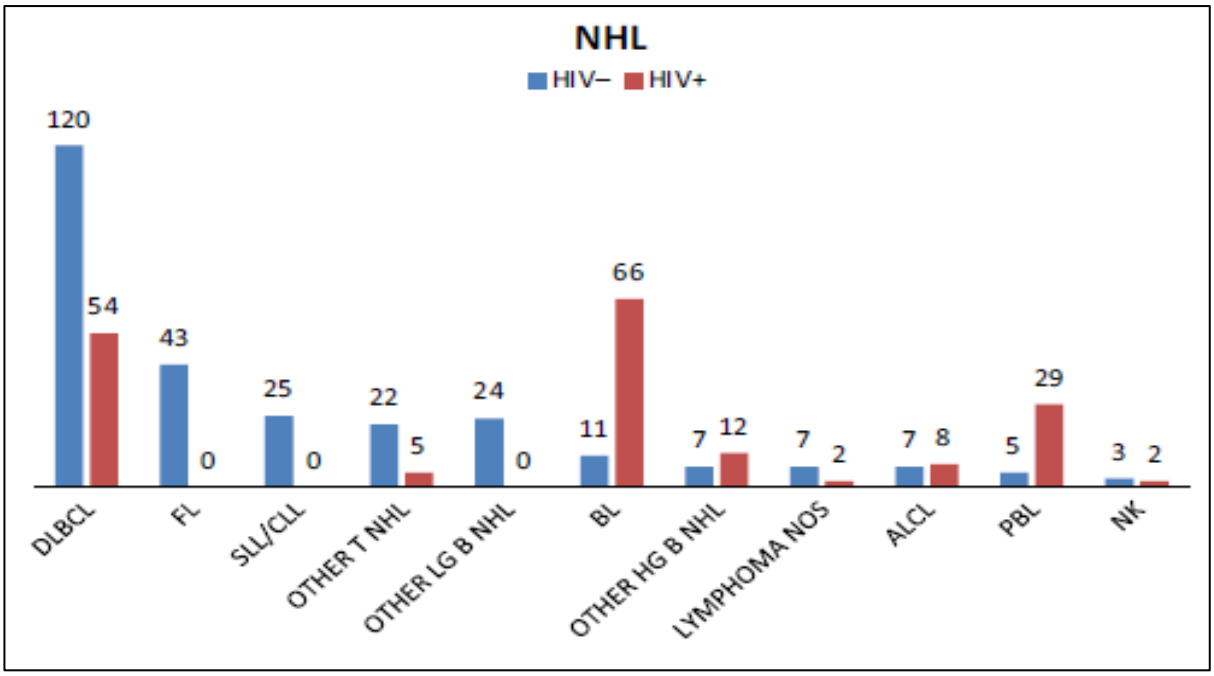

Figure 1.1: Bone Marrow Biopsies of in NHL HIV-Positive and HIV-Negative Patients. The graph depicts distribution of NHL subtypes by HIV status from patients undergoing bone marrow biopsies at Groote Schuur Hospital (2005-2010). DLBCL : Diffuse Large B-cell Lymphoma; FL : Follicular Lymphoma; SLL/CLL : small lymphocytic lymphoma/chronic lymphocytic leukaemia; LG B NHL, Low Grade Burkitt Lymphoma; HG-B NHL High Grade Burkitt Lymphoma; NOS :Not Otherwise Specified; ALCL : Anaplastic Large Cell Lymphoma; PBL : Plasmablastic Lymphoma; NK : Natural Killer Cell Malignancy [19].

2005-2010 from patients under investigation at Groote Schuur Hospital in Cape Town show NHL to be the most frequently detected malignancy among HIV positive patients, with Burkitt Lymphoma (BL), Diffuse Large B-cell Lymphoma (DLBCL) and Plasmablastic Lymphoma (PBL) being the most prevalent (Figure 1.1). This is in line with data from other studies performed elsewhere in the world, with several of those reporting a persisting elevated incidence of HIV-associated NHL among HIV infected individuals despite the introduction of combination antiretroviral therapy [8, 12, 19, 24]. In particular, studies have shown that the highly aggressive Burkitt lymphoma can occur in HIV positive patients even when CD4 cell counts are within a healthy range [108].

1.2.1 Burkitt Lymphoma (BL)

BL is a High-Grade B-cell NHL that is frequently present in extra-nodal sites or as acute leukaemia. In 1958, Denis Burkitt was the first to clinically

describe the lymphoma based on the high proportion of reported cases involving the development of abnormal jaw tumours and abdominal tumours amongst Ugandan children [109]. The World Health Organization (WHO) further subdivides BL into three clinical variants based on a variety of factors such as clinical presentation; molecular genetics and differences in geographical distribution: The three variants include: Endemic, Sporadic and Immunodeficiency-related. Endemic BL is mainly prevalent amongst children and occurs predominantly in Equatorial Africa, particularly within areas associated with Malaria and early infection with the Epstein-Barr virus (EBV). Sporadic BL occurs throughout the rest of the world, accounting for 30-40% of childhood NHL cases but is also seen in young adults. Immunodeficiency-related BL occurs predominantly in HIV positive individuals, and persistent B-cell activation, due to infection with the virus, has been attributed to this phenomenon [20, 109].

The cell of origin seems to vary based on the clinical variant of BL. For Sporadic BL, which normally is EBV negative, the cell of origin is postulated to be a mature, yet highly proliferative B-cell present within the dark zone (DZ) of the germinal centre (GC), undergoing somatic hypermutation during

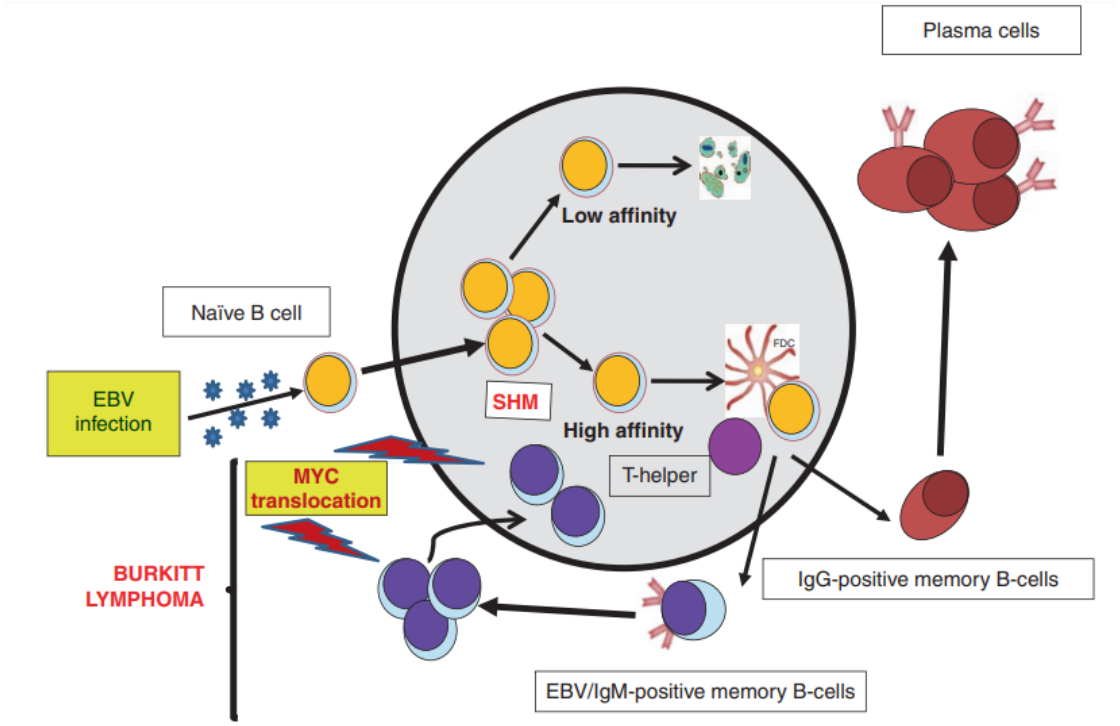

Figure 1.2: Model for the postulated cell of origin for Burkitt Lymphoma [109].

the GC reaction (Figure 1.2). However, this does not account for any EBV-associated BL cases. In these cases, the cell of origin is suggested to be post germinal centre B-cells (memory B-cells), which are considered to be in a later stage of development. [109].

Immunophenotyping of BL reveals that tumour cells are normally positive for membrane IgM; B-cell antigens (CD19, CD20, CD22, CD79a, PAX5) and GC markers (CD10, BCL-6). CD38, CD77, and CD43 are also frequently positive. In addition to this, the expression of CD38, CD77, and CD43 are often detected with the expression of BCL-2, an anti-apoptotic protein, being absent. Majority of BL cases also present a high expression of the proto-oncogene *c-MYC* in most cells, despite the absence of the c-MYC/IgH translocation in some cases [109].

BL cells consists of monomorphic medium sized round B-cells with basophilic cytoplasm with the cytoplasmic margins appearing squared off. The nuclei appear round or oval in shape and contain coarse, clumped chromatin and deeply basophilic nucleoli (Figure 1.3A). In terms of histopathology, BL cells appear to be arranged within a characteristic “starry sky” pattern (Figure 1.3A). This pattern most likely resulted from the presence of phagocytic histiocytes, such as macrophages, which actively phagocytose nuclear debris from BL cells experiencing a high level of apoptosis. Despite the high proliferation index, a major portion of BL cells will undergo apoptosis. BL tissue displaying an abnormal morphology (plasmacytoid appearance) commonly associated with adult and HIV positive patients (Figure 1.3B) [20, 21, 109].

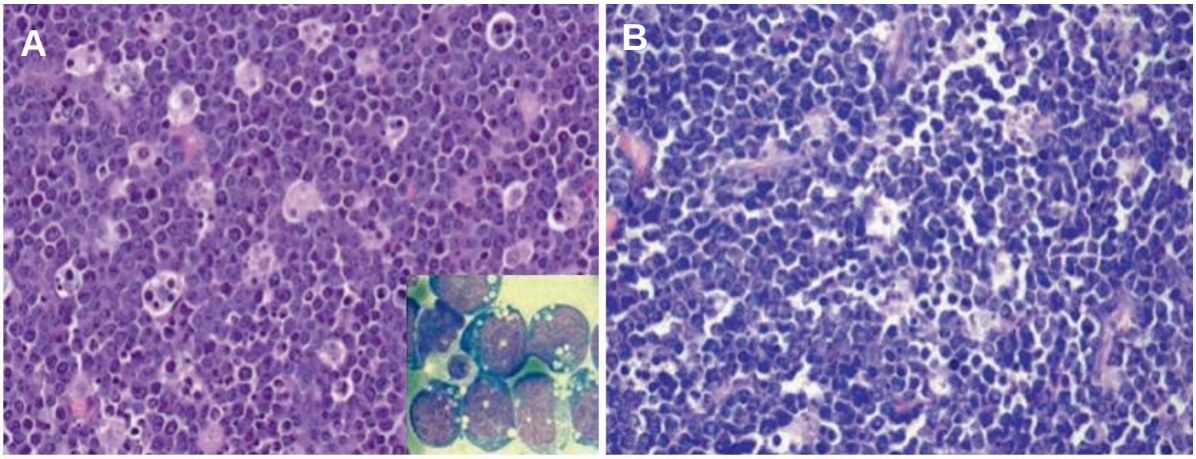

Figure 1.3: The cellular morphology and histology of Burkitt Lymphoma tissue (Haematoxylin and Eosin Stain). (A) Typical morphology of BL tissue displaying the characteristic "starry sky" pattern. (B) The abnormal morphology, depicting a plasmacytoid appearance, that may be present in adults that are HIV positive [109].

Several co-factors are associated with BL and will influence its epidemiology. These include the presence of an EBV infection, prevalence of Malaria and HIV infection. Of note to this study is the effect of HIV infection on the incidence of BL (HIV-associated BL).

1.2.1.1 HIV-associated BL

As mentioned earlier, BL is one of the HIV-associated cancers that is overrepresented within the South African HIV population. An enhanced risk of BL has been shown to be linked with chronic HIV infection. Chronic HIV infection has been reported to cause persistent activation of B-cells, indicated by the increased proportion of specific B-cell activation markers such as CD30 and CD23 reported within the serum of HIV positive patients. Persistent stimulation of B-cells results in the overexpression of the enzyme Activation Induced Cytidine Deaminase (AID). The virus is thought to use this mechanism to promote the risk of HIV-associated lymphomas such as BL [20, 109]. Therefore, studies to understand this mechanism is ongoing. Furthermore, the overexpression of AID, a key driver of antibody diversification in B cells, has been shown to be essential in the translocation of proto-oncogene *c-MYC* to the highly active immunoglobulin heavy (IGH) locus (*c-MYC/IgH* translocation, t(8;14)(q24;q32)), a defining feature of BL cells. The persistent activation of B-cells has been shown to be one of the ways via which AID is overexpressed. Furthermore, co-infection with EBV or even

the presence of specific cytokines have been shown to promote the survival of chronically activated B-cells with *c-MYC* translocation, thus promoting lymphomagenesis [19, 20, 21].

Despite HIV being a typical risk factor for the development of HIV-associated BL, it might not be the only factor responsible as BL has been reported to develop in patients with normal CD4 cell counts. Furthermore, the incidence of HIV-associated BL was not observed to increase as the CD4 cell count decreases or in patients that are not on Antiretroviral Treatment (ART) [123].

1.3 The Oncogenic Role of HIV

The high incidence of HIV-associated cancers, such as BL, amongst HIV positive patients was initially thought to be associated with the immunosuppressive role of the virus [24]. The commencement of ART has allowed for successful repression of the virus and a greater life expectancy amongst HIV positive patients. However, they continue to experience persistent immune activation and chronic inflammation (such as persistent B-cell activation), potentially making them more vulnerable to developing numerous complications such as cancers as they age [7, 61]. In addition to this, the introduction of ART caused no reduction in the incidence of BL in HIV positive patients compared to other HIV-associated NHL such as DLBCL and CNS lymphoma [123]. However, in the last decade new research has emerged which show that specific proteins encoded by the virus can directly drive oncogenic processes within cells, and these include non-HIV host cells. One study has shown that HIV protein can travel from HIV-infected macrophages into B cells via specialised conduits [16]. Other studies indicate that HIV soluble proteins are present in the serum of HIV infected patients, and that these proteins can alter cellular processes through binding to membrane receptors [33]. To promote oncogenesis, HIV proteins have been shown to either act alone or collaboratively with cellular proteins, as well as with oncoproteins of established oncogenic viruses such as the Kaposi's Sarcoma-associated Herpes Virus (KSHV), or with EBV [14, 15, 24, 25, 33, 34].

One of the HIV-1 proteins which has been most commonly described as having oncogenic potential is the HIV Trans-activator of Transcription protein (Tat). This regulatory protein, whose normal role is in enhancing the efficiency of viral transcription [31], has been shown to play a key role in the progression of Kaposi Sarcoma in HIV infected individuals. Tat was shown to cooperate with ORF-K1 (an oncogenic viral protein of KSHV) to co-induce the expression of micro-RNA miR-891a-5p, which in turn upregulates NF-κB, indirectly resulting in the induction of abnormal angiogenesis [26]. Another more recent study reported that Tat interacts with LINC00313, a KSHV reactivation-activated long noncoding RNA (lncRNA). Normally, LINC00313 is upregulated during KSHV infection which in turn blocks cell migration and invasion. However, the presence of Tat abolishes this effect, thus potentially enhancing KS progression [55]. Within the context of lymphoma, Tat has been shown to play an important role in inducing BL-specific chromosomal translocations within B-cells such as the t(8;14) chromosomal translocation mentioned earlier (see section 1.2.1), thereby increasing the risk of BL in HIV positive patients. Tat was reported to achieve this by firstly enhancing the co-localization between the c-*MYC* and *IgH* genes and secondly increasing the expression of AID, which causes the emergence of double-stranded breaks within the *c-MYC* and *IgH* genes of naïve B-cells. In Ramos cells (a BL cell line) expressing HIV-1 Tat, the viral protein was reported to interact with the AID gene (*AICDA)* via three regulatory regions (R1, R2 and R4), resulting in enhanced AID protein expression. In addition to this, Tat also enhanced the activity of the *c-MYC* promoter, which correlated with increased levels of the c-MYC protein in Ramos cell [14, 32, 110]. Furthermore, another study reported that Tat was present within the sera of HIV infected patients that presented with B-cell lymphomas such DLCBL and BL. This would suggest that Tat is able to act as a biologically active extracellular protein, released from infected cells and potentially taken up by uninfected B-cells [28].

A second HIV protein shown to have direct oncogenic function is the matrix protein p17 whose normal role is in regulating viral entry and replication. Several studies reported on the ability of p17 to enhance cellular features which have the potential to promote a cancer phenotype. Of note is a study

by Martorelli and colleagues who demonstrate that a natural variant of p17 (S75X) could bind to the CXCR2 receptor on EBV-infected B-lymphocytes more efficiently than the reference p17 protein, and that this led to enhanced proliferation. The p17 variant could upregulate the oncogenic EBV viral protein Latent Membrane Protein-1 (LMP-1), and enhance PI3K/AKT, MAPK/ERK1/2 and STAT3 signalling [34].

Of note to this study is the oncogenic function of HIV Nef, and the next section presents data currently available on the involvement of Nef in carcinogenesis.

1.3.1 The Role of HIV-1 Negative Factor (Nef) protein in cancer

1.3.1.1 HIV Nef in Viral Infection

The HIV-1 Nef protein is a 27-kDa myristoylated protein that is abundantly expressed during early stages of infection. The Nef protein contains three structural domains which include the folded (globular) core (residues 55-65 and 84-203) flanked by the N-terminal (residues 1-54) and C-terminal disordered loop domains (residues 204-206). A central flexible loop (residues 149-179) is present within the folded core (Figure 1.4 below) [38, 39]. Each section contains amino acid residues imperative for its multifunctional capabilities, despite showing no evidence of enzymatic activity. Each structural domain will contain different Nef protein motifs, which effectively allows Nef to carry out many of its functions. For example, the proline rich

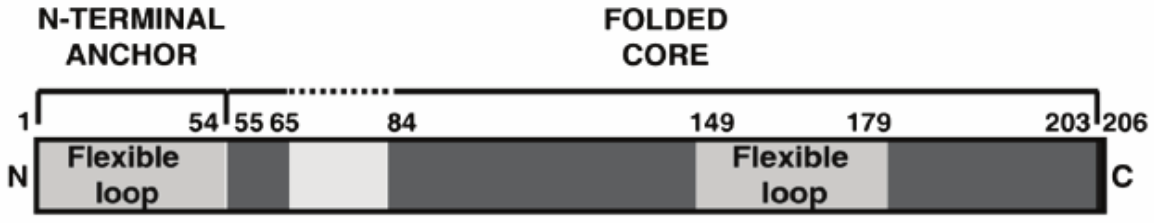

Figure 1.4: A schematic diagram of the HIV-1 Nef protein depicting its structural domains: N-terminal (residues 1-54); Folded Core (residues 55-65 and 84-203); C-terminal (residues 204-206) and central flexible loop (residues 149-179) within the folded core [39].

motif PxxPxR, found within the core of Nef, plays a role in modulating T-cell activation by mediating an interaction between the Nef protein and the SH3 domain of various Src family tyrosine kinases such as Hck [37, 38, 39, 91]. ExxxLL, an acidic di-leucin motif located within the C-terminal loop, allows

the Nef protein to interact with various proteins involved in intracellular trafficking such as the Adaptor Protein-2 (AP-2), which in turn will produce endosomes containing CD4 and Nef. In addition to this, the motif has also been reported to regulate various cell surface molecules such as CD4. The Nef protein also contains $MGxxxS_{(1)}$, a myristoylated motif within the N-terminal, which is a protein lipid modification which acts as a membrane-anchoring motif allowing Nef to be localized and inserted into the cell membranes of target cells. This is also critical for the downregulation of certain cell surface molecules such CD4 and Major Histocompatibility Complex I (MHC-I) [37, 38, 41, 91].

Nef is involved in optimization of viral infection through mechanisms that are not completely understood but most likely involves the protein interacting with various host cellular factors allowing for disruption of intracellular trafficking and alteration in the expression of certain cell surface molecules. For example, Nef has been shown to interact with and subsequently downregulate (via endocytosis) the CD4 receptor molecule on the cell surface of T-cells. This reduction of the HIV target receptor prevents superinfection thus favouring viral propagation [38-41]. Nef has also been shown to promote viral dissemination by preventing the elimination of infected cells through downregulation of surface MHC-I via endocytosis, thus ensuring the extended survival of infected T-cells and circumvention of the host's immune system [41-43].

1.3.1.2 The Role of HIV Nef in cancer

An oncogenic role for HIV Nef has been demonstrated in several cancer types. For instance, in KS, Nef was shown to enhance KSHV K1-induced angiogenesis via an alternative mechanism to Tat. Nef and ORF-K1 were shown to collaborate to enhance KS angiogenesis by both inducing the expression of micro-RNA miR-718, an inhibitor of PTEN, thereby allowing for the AKT/mTOR signalling pathway to be synergistically upregulated, enhancing KS angiogenesis [25]. Furthermore, Nef demonstrates another role in promoting KS through its interaction with KSHV viral Interleukin-6 (vIL-6) Without the presence of Nef, vIL-6 has been confirmed to display certain

oncogenic properties such as the activation of angiogenesis and tumorigenesis *in vitro* (in endothelial cells and fibroblasts) and *in vivo* (chicken chorioallantoic membrane or CAM model and Nude Mice models). However, when Nef was present (exogenous or ectopic expression), it was reported to synergize with vIL-6 to enhance its oncogenic properties, such as angiogenesis and tumorigenesis, through induction of the AKT signalling pathway [54].

A study done by Santerre and colleagues demonstrated that HIV-1 Nef led to a more aggressive phenotype in Non-Small Cell Lung Cancer (NSCLC) [72]. NSCLC cells ectopically expressing the viral protein displayed enhanced cellular proliferation as well as increased angiogenesis and decreased expression of the tumour suppressor protein p53 [72]. Furthermore, Nef has been shown to enhance cellular proliferation in various other cell types such as resting $CD4^+$ T cells and TF-1 cells (human macrophage precursor cell line) [50, 85].

Another cancer hallmark that Nef has been linked to is the inhibition of apoptosis. The N-terminal (residues 1-54; Figure1.4) of Nef protein has been shown to have the ability to directly interfere with p53, effectively blocking p53-dependent apoptosis of MOLT-4 cells (human leukaemia CD4-expressing T-cell line) [90]. The full length Nef was shown to block apoptosis of T-cells through activation of the p21-activated kinase (PAK) using phosphatidylinositol 3-kinase (PI3K), which in turn results in the phosphorylation and subsequent inhibition of the pro-apoptotic protein Bad, stimulating pro-survival signalling [111]. In the TF-1 cell line, Nef was shown to signal via the ERK/MAPK pathway, resulting in an increased expression of the anti-apoptotic gene, *Bcl-X_L,* effectively switching apoptosis off [50].

Autophagy, a cellular process that plays a role in both tumour suppression and promotion, has also been linked to Nef. Specifically, the viral protein was shown to block the progression of autophagy by preventing the fusion of the autophagosome to lysosome and was also reported to block its activation by disrupting the conversion of autophagy-related protein LC3-I to LC3-II. Considering this, its plausible that Nef could potentially be driving

tumorigenesis by disrupting autophagy as its dysregulation has long been associated with cancer [48, 95].

B-cells are not natural hosts for HIV, however, a study by Xu *et al.* demonstrated that HIV Nef can be shuttled into B-cells from infected macrophages via conduits/protrusions that specifically targets and adheres to nearby B-cells (Figure 1.5) [37].

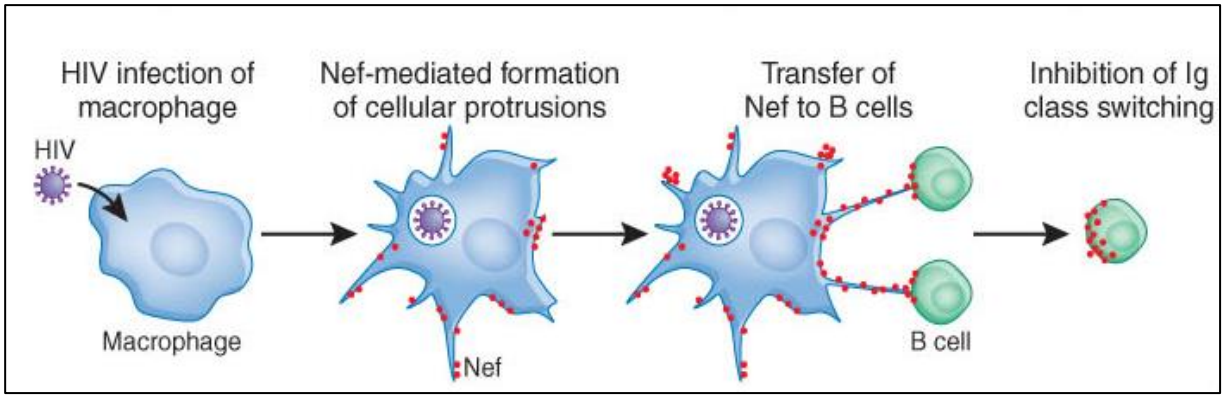

Figure 1.5: HIV-1 infected macrophages will form intercellular conduits or cellular protrusions, which allow the Nef protein to be trafficked to B-cells. Diagram depicting the potential mechanism utilized by HIV-1 Nef protein to transfer to B-lymphocytes. Once inside B-cells, Nef will go on to disrupt many biological processes, (for example: the inhibition of Ig Class Switching) which all could potentially drive B-cell lymphomagenesis [37, 69].

Besides the membrane-bound myristoylated conformation of Nef, a cytosolic version of the protein exists and has been reported to alter certain biological process within macrophages by binding to MHC II class receptors and the trans-Golgi network. Both membrane and cytosolic forms can make use of the cellular protrusions to be transferred to B-cells, therefore allowing Nef to instigate many B-cell damages via the interference of several biological processes, possibly promoting B-cell lymphomagenesis [16, 37]. A study done by Swingler, and colleagues reported that Nef-expressing macrophage supernatants were potentially able to induce B-cell proliferation indirectly via the secretion of ferritin by infected macrophages [86, 87].

Lamers and colleagues proposed that the Nef protein could possibly be initiating B-cell activation, resulting in the overexpression of the *AICDA* gene, by stimulating infected macrophages to excessively produce anti-inflammatory cytokines. Furthermore, the overexpression of the *AICDA* gene in turn could potentially result in the advent of oncogenic chromosomal rearrangements (MYC-immunoglobulin gene loci), thus promoting

lymphomagenesis. However, the mechanism surrounding this remains undetermined and demands further exploration [16, 17, 37].

Overall, the potential phenotypic changes brought on by HIV-1 Nef in B-cells and their possible contribution to lymphomagenesis have not been extensively explored. Therefore, more work must be done to further investigate and understand the role of HIV-1 Nef in B-cell lymphomas, such as BL. This continues to be the topic of investigation in our laboratory with the next section describing some the preliminary data generated.

1.4 Preliminary Studies and Aims of current study.

Previous work in our laboratory, aimed at defining the role of HIV Nef in B-cell lymphoma, specifically, in Burkitt lymphoma, found that the protein could influence key cellular processes, potentiating enhanced carcinogenesis in lymphoma cells.

The extracellular exposure of BL cells to recombinant Nef protein led to enhanced expression of two key lymphoma promoting factors, namely c-MYC and AID, in these cells. This occurred at both the transcriptional and protein levels (Figure 1.6) [52]. Furthermore, Nef exposure led to increased recruitment of phosphorylated γ-H2AX, a factor which gets recruited to the site of Double-Stranded Breaks (DSBs), to the DNA of the lymphoma cells, indicative of increased genomic instability (Figure 1.7). The latter is known to be a precursor for chromosomal translocations which is a hallmark feature of haematopoietic malignancies including BL.

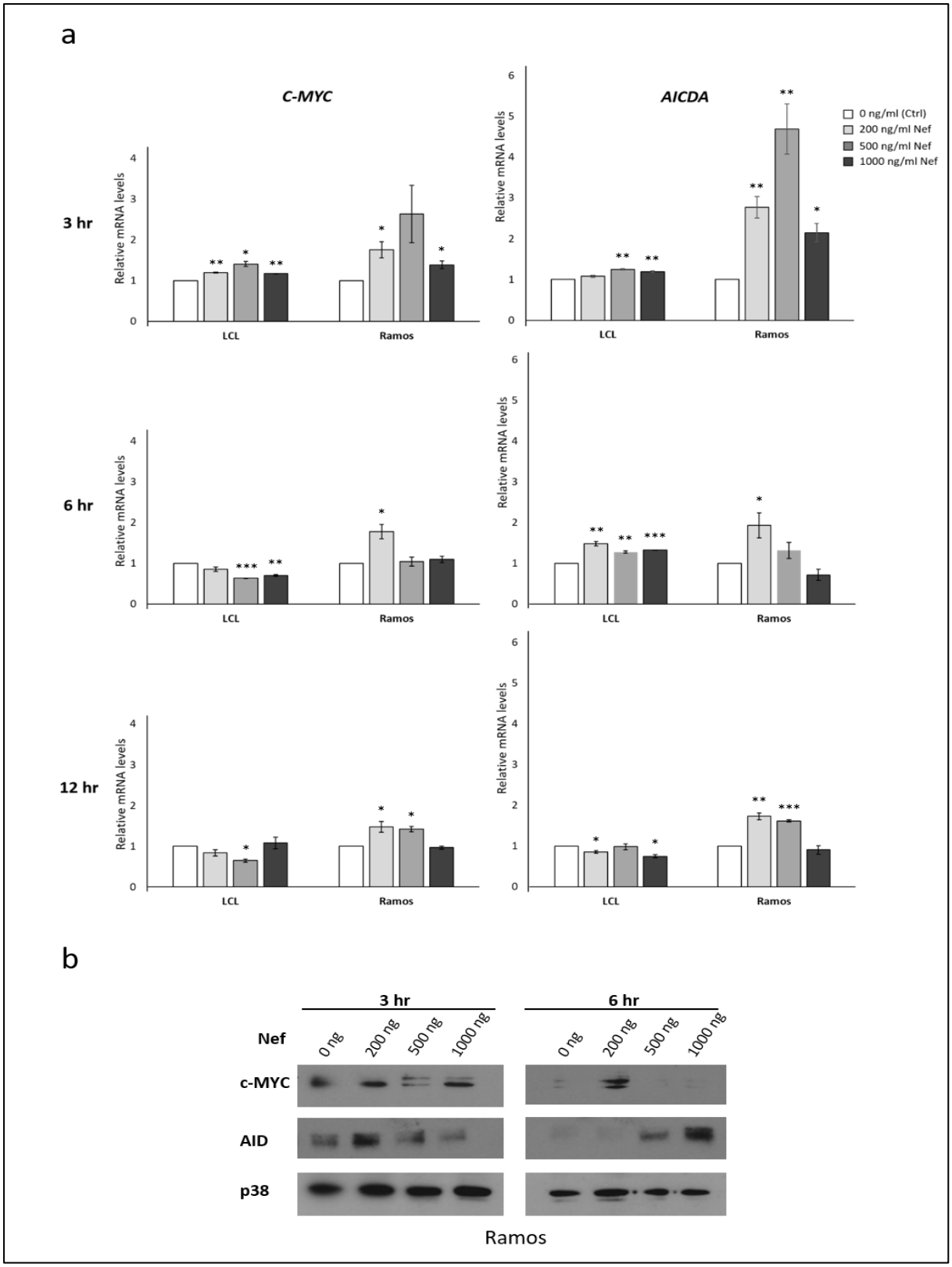

Figure 1.6: AID and c-MYC expressions are altered in B-cells upon exposure to HIV Nef. (A) Bar graphs showing relative mRNA expression of *c-MYC* (left panel) and *AICDA* (right panel) at 3 hr, 6 hr and 12 hr exposure to HIV Nef, in lymphoblastoid cells (LCL) and Burkitt lymphoma cells (Ramos). The levels were normalised to the internal control *GAPDH* and plotted relative to mock (0 ng/ml) treated cells. *** p≤0.001; **p≤0.01; * p≤0.05. All experiments were performed in triplicate. (B) Western blot of whole protein extracts from Ramos cells exposed to extracellular Nef at the indicated concentrations

(ng/mL) for the indicated times. p38 was detected as a loading control. All experiments were performed in triplicate [52].

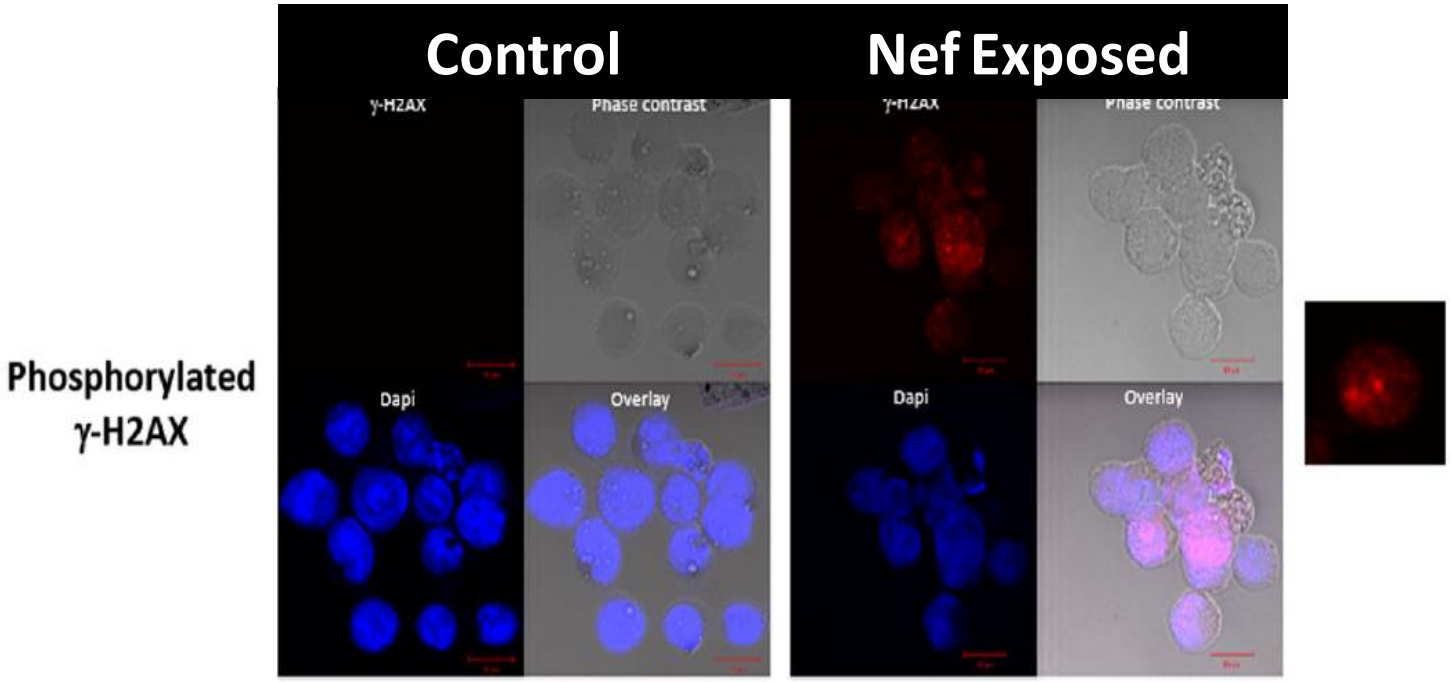

Figure 1.7: Extracellular exposure to recombinant HIV Nef led to an increased expression of γ-H2AX in lymphoma cells, indicating enhanced genomic instability. Ramos cells were extracellularly treated with 500 ng/ml of recombinant Nef protein for 3hr. After exposure, cells were fixed and permeabilized. The presence of c-MYC, AID and γ-H2AX were detected with specific primary antibodies and fluorescently tagged (Cy3 - red) secondary antibodies. DNA was stained with DAPI (blue). Cells were mounted on slides and images were captured using confocal microscopy. Left hand panel: Mock-treated/Control; Right hand panel: treatment with recombinant Nef protein; Far-right hand side: Enlarged image of one representative Ramos cell from treated group [52].

The current project is aimed at further exploring the oncogenic effects of HIV-1 Nef protein on BL cells using specific cellular assays. Furthermore, the possible internalization of the Nef protein by B-cells during extracellular exposure will be explored.

Therefore, the objectives of the current study are:

- To measure the effect of HIV-1 Nef on BL cell proliferation
- To assess the impact of HIV-1 Nef exposure on the expression of cyclins and the cell cycle profile in BL cells
- To measure changes in apoptosis in cells exposed to HIV-1 Nef, in the presence and absence of a chemotherapeutic insult
- To explore the potential internalization of HIV-1 Nef by BL cells.

Chapter 2

Methodology

2.1 Tissue Culture

2.1.1 Cell Lines and Storage

The Burkitt Lymphoma (BL) cell line Ramos was purchased from the American Type Culture Collection (ATCC®, Virginia, USA) and the BL cell line BL-41 was kindly donated by Professor Dave Sandeep, from Duke University (North Carolina, USA). Both cell lines are negative for EBV infection. The HT1080 cell line is originally derived from a fibrosarcoma and kindly donated by Professor Sharon Prince (Department of Human Biology, University of Cape Town).

Both Ramos and BL-41 cell lines were cryopreserved in freezing media containing 10% dimethyl sulfoxide (DMSO), Roswell Park Memorial Institute (RPMI) media (Sigma Aldrich, Missouri, USA); Fetal Bovine Serum (FBS) (Appendix A) and stored in liquid nitrogen. The HT1080 cell line was cryopreserved in freezing media containing 10% DMSO, Dulbecco's Modified Eagle Medium (DMEM) media (Sigma Aldrich, Missouri, USA); Fetal Bovine Serum (FBS) (Appendix A).

2.1.2 Thawing, Expansion and Freezing

For suspension cell lines (Ramos and BL-41), complete growth media was first prepared by combining RPMI-1640 media (Sigma Aldrich, Missouri, USA); 10% FBS and 1% Penicillin/Streptomycin (P/S) (Appendix A). One vial of cryopreserved cells was removed from liquid nitrogen, thawed and added to pre-warmed growth medium in the 15 ml Falcon tube. The cells were then pelleted in order to remove the toxic DMSO. The pellet was then resuspended in 1 ml of the warmed media and added to a T25 flask, containing an additional 5 ml of media, which was then placed in the incubator (5% CO_2, 37°C). Ramos and BL-41 cells were maintained and expanded by adding fresh

growth media every 2-3 days and depopulated as needed. The cells grew best and were maintained at a density of between 2 X 10^5 and 1 X 10^6 viable cells/ml.

For adherent cell lines (HT1080), cells were thawed in a similar process, as described above, with the exception being the completed growth media used which consisted of DMEM (Sigma-Aldrich, USA) containing 10% FBS and 1% Penicillin/Streptomycin (P/S) (Appendix A). Cells were resuspended in 1 ml of media and transferred into a 10 cm tissue culture dish containing 9 ml of media, previously warmed to room temperature (RT). The dish was agitated gently and then incubated in the CO_2 incubator (5% CO_2, 37°C). When the HT1080 cells reached ~80% confluency, the dish was removed from the incubator and media suctioned off. Cells were trypsinized by adding 1 ml of 1X Trypsin-EDTA (Appendix A) to the dish. The dish was incubated at 37°C for 3 minutes or until the cells were detached from the base of the plate. Thereafter, 1 ml of complete media was added to inactivate the trypsin, and the cell resuspension was transferred to a new 10 cm dish containing 9 ml of complete media. The dish was then incubated in the CO_2 incubator (5% CO_2, 37°C).

In terms of freezing suspension cells, cryomedia consisting of RPMI (Sigma Aldrich, Missouri, USA), 10% FBS and 10% DMSO (cryoprotective agent) (Appendix A) was prepared and place on ice (in the fume hood). The expanded cells were counted (using a Haemocytometer), pelleted and resuspended in the cryomedia (the final density of the cell suspension was approximately 1 X 10^6 cells/ml). The cell suspension was added to cryovials (1 ml/vial), which were then placed in a freezing container with isopropanol at -80°C overnight. The cryovials were transferred into liquid nitrogen for long term storage the following day. A similar process was employed for adherent cells with some alterations. The cryomedia prepared contained DMEM (Sigma Aldrich, Missouri, USA), 10% FBS and 10% DMSO (Appendix A). Adherent cells were trypsinized (as described above), counted, pelleted and resuspended in cryomedia. Once resuspended, the cell suspension was distributed to

cryovials (1 ml/vial) and placed in liquid nitrogen using the same method described for Ramos and BL-41 cells above.

2.1.3 Transfection of HT1080 cells to generate a Nef-expressing control.

2.1.3.1 Plating of HT1080 cells

16 hours prior to transfection, HT1080 cells were plated to ensure a confluency of 70-80% on the day of transfection. To achieve this, cells were lifted using Trypsin-EDTA (Appendix A), transferred to a 15 ml sterile tube, diluted appropriately and counted using a Haemocytometer. Cells were then plated in low serum media (media supplemented with 0,5% FBS and 1% P/S) (Appendix A) at a concentration of $3,5\times10^5$ cells/ml in 35 mm cell culture dishes and placed in the CO_2 incubator overnight.

2.1.3.2 Transfection

Transfection of HT1080 cells were performed using the X-tremeGENE HP DNA Transfection Reagent (Roche, SA) in accordance with the manufacturer's instructions. Briefly, 2 µg of pcDNA3.1-Nef, an HIV-1 Nef mammalian expression vector (kindly donated by Professor Mitra, National Centre for Cell Science, India) isolated using a method which has an endotoxin-removal step, was mixed with 2 µl of XtremeGENE HP diluted in 200 µl of DMEM only, as per the manufacturer's guidelines. Following a 30 minute incubation at RT to allow for the transfection reagent (TR)/DNA complex to form, the mixture was added dropwise to the cells. A control plate was also generated, which did not contain plasmid DNA. Both plates were incubated at 5% CO_2 for 30 hours.

2.1.3.3 Harvesting

Approximately 30 hours post-transfection, the cell lysates were harvested in the 2X Boiling Blue extraction buffer (Appendix A). The dishes were placed on ice, the medium was aspirated off and the cells washed twice with 1 ml of ice-cold 1XPBS (Appendix A). The cells from each well were scraped in 70 µl of 2X Boiling Blue using a 1 ml syringe plunger, transferred into 1,5 ml

microcentrifuge tubes, boiled for 5-10 minutes and stored at -20°C until further use.

2.1.4 Mycoplasma Testing

All cell lines were tested for mycoplasma contamination prior to receiving any treatments. Cells (1 X 10^6 cells/ml) were cultured in antibiotic free complete media for at least 48 hours prior to the test. Approximately 3 µl of cell suspension was deposited directly on a sterilised microscope slide and allowed to air dry before being fixed for 2 minutes using the fixative (enough to cover the cells) (Appendix A). Cells were thereafter washed with distilled water and stained with Hoechst stain reagent (0,5 µg/ml) (H33342; Sigma Aldrich, MO, USA) for 5-8 minutes. The stain was removed, and the cells were washed with distilled water with excess water being blotted out using tissue paper. Next, a drop of mounting fluid (Appendix A) was added to the cells before covering with a clean cover slip. The cells were viewed by fluorescent microscopy at 40X magnification using the Zeiss Axiovert Fluorescence Microscope (Carl Zeiss Microimaging, Germany).

2.1.5 Cell Treatments

Recombinant Nef protein treatment: Ramos and BL-41 cells were counted using a haemocytometer and plated ($3,5\times10^5$ cells/ml) approximately 16 hours prior to treatment in low serum medium (Appendix A). The cells were treated with either the recombinant HIV-1 Nef protein at the appropriate concentrations which was made by diluting the stock (1 mg/ml) (NIH AIDS Research and Reference Reagent Program, USA; HIV-1 HXB2 Nef Recombinant Protein cat# 13134) or left untreated (control). The treatment times varied, depending on the assay.

Doxorubicin treatment: This treatment was used to induce apoptosis in Ramos cells, while investigating the potential anti-apoptotic effect of HIV-1 Nef on cells. Ramos cells were plated in low-serum medium as described above and treated with 0,35 µg/ml Doxorubicin Hydrochloride (Sigma Aldrich, Missouri, USA; Product No. D1515; stock concentration: 250 µg/ml) for 24 hours. The assay is described in more detail in Section 2.4 below.

2.1.6 Cell Viability Assay

2.1.6.1 SDS-PAGE

Before conducting the WST-1 assay, the integrity of the recombinant Nef proteins were first assessed. Protein samples were then separated using an SDS-PAGE (sodium dodecyl sulphate-polyacrylamide gel electrophoresis) to separate proteins by molecular weight. In accordance with the manufacturer's instructions, a 1.5 mm 15% resolving gel (Appendix A) and a 5% stacking gel (Appendix A) was prepared using the Mini-PROTEAN 3 casting apparatus (Bio-Rad, California, USA). All samples were prepared and heated to 95°C for 5 min to denature the protein and centrifuged briefly prior to loading on the polyacrylamide gel. Samples were loaded into the wells of the gel which was assembled in the gel-running apparatus, as per manufacturer's instructions. 5 µl of the BenchMark™ Pre-stained 1 Kb Protein Ladder (Figure B1, Appendix B) was loaded into at least one well and 5 µl of 5X SDS loading dye (Appendix A) being loaded into any empty wells to ensure proteins separate evenly. The tank was then closed and connected to the Bio-Rad Power pack 200 and the gel was electrophoresed for 2-2.5 hours at 100 volts (until the dye front reached the bottom of the gel).

2.1.6.2 Visualization using Coomassie blue

After the proteins have been separated on the gel, Coomassie blue (Appendix A) was used to stain the protein bands in the gel by incubating the gel in the stain at RT overnight with gentle agitation. Next, destaining solution (Appendix A) was added to the gel, accompanied by gentle agitation, and was continuously discarded and replaced with fresh destaining solution till the protein bands were clearly visible on the gel without any background staining. Gels were then transferred into distilled H_2O.

2.1.6.3 WST-1 Assay

To investigate changes in the proliferation of BL cell lines (Ramos and BL-41) in response to treatment with recombinant Nef protein, a viability assay was performed using the WST-1 cell proliferation reagent (Roche Applied Science,

Penzberg, Germany). The WST-1 reagent is a tetrazolium salt that is normally cleaved by mitochondrial enzymes, produced by metabolically active cells, to form a soluble formazan dye. Therefore, the amount of formazan dye formed directly correlates to the number of metabolically active cells in the culture. The more salt that is cleaved, the greater the colour change, which serves as an indirect indicator of cellular viability [96].

Approximately 16 hours prior to treatment, cells were counted using a haemocytometer and plated in low-serum media (0,5% FBS) at a concentration of $3,5\times10^5$ cells/ml in 12-well plates. Culture media containing no cells was also included to serve as a blank/background for the viability assay. Cells were treated with recombinant Nef protein at the following concentrations: 0; 50; 100; 200 and 400 ng/ml for 3; 6 and 24 hours. Controls were left untreated as the Nef protein was diluted in RPMI and the volume of Nef used was very small – less than 10 µl . Thus, it was not deemed necessary to add diluent to the control plates. At the end of treatment, 100 µl of cell suspension (or background control) was added to a 96-well plate, followed by 10 µl of WST-1 reagent. The plate was then covered in foil and placed in a CO_2 incubator for 2 hours (37°C; 5% CO_2) before colourimetric analysis using the spectrophotometer function of the Glo-Max®-Multi+ multiplate reader (Promega, Wisconsin, USA) at a wavelength of 450 nm. The experiments were repeated at least three times for both cell lines.

2.2 Protein Extraction, Quantification and Western Blotting

2.2.1 Protein Extraction

Total soluble protein extraction was performed using Radio-Immunoprecipitation Assay (RIPA) buffer (Appendix A) combined with 7X complete™, mini EDTA-free Protease Inhibitor (Appendix A) (Roche Applied Science, Penzberg, Germany). The RIPA buffer contains specific detergents which effectively lyse and permeabilise the cells while the Protease Inhibitor prevents degradation of extracted proteins. At the time of extraction, fresh RIPA/Protease Inhibitor extraction buffer was made and kept on ice. Cells

were transferred to 15 ml Falcon tubes, pelleted by centrifugation at 2000 rpm for 5 min, with the resulting pellets being washed twice in 1 ml of cold 1XPBS before being transferred to a 1.5 ml microcentrifuge tube for the final PBS wash. The amount of extraction buffer added was determined by the pellet size. Generally, 70 µl of the RIPA/Protease buffer was used to resuspend the cell pellet. Thereafter, the suspension was incubated at -80°C overnight to optimise cell lysis before spinning at high speed (12 000 rpm at 4°C) for 20 minutes. The resulting supernatant, containing the soluble proteins, was then transferred in aliquots to fresh tubes and stored at -80°C until use.

2.2.2 Protein Quantification using BCA

To determine the concentration of the total protein in each sample, a Bicinchoninic acid (BCA) assay was performed using the Pierce™ BCA Assay kit (Thermo Fisher Scientific™, Massachusetts, USA). The BCA assay utilises a specific colourimetric system based on the Biuret reaction. This involves the reduction of Cu^{+2} to Cu^{+1} by the protein peptide bonds in an alkaline environment. BCA molecules will then chelate with the reduced Cu^{+1} cations to form a BCA/Cu^{+1} complex, resulting in a purple colour being produced which is proportional to increasing protein concentrations [97].

Briefly, the protein samples were thawed on ice and diluted into a ratio of 1:5 using the RIPA buffer (total volume of 25 µl) or kept undiluted. The BCA working reagent was prepared according to the manufacturer's protocol by mixing reagents A and B in a ratio of 50:1. A standard curve was generated using the Bovine Serum Albumin (BSA) standards at a range of concentrations (2000 µg/ml, 1000 µg/ml, 500 µg/ml, 125 µg/ml and 0 µg/ml) (RIPA buffer blank). In a 96-well plate, 10 µl of each diluted protein sample as well as the standards were added to wells in duplicates, followed by 200 µl of the working reagent. The plate was then incubated at 37°C for 30 minutes with the resulting colour changes being measured using the Glo-Max®-Multi+ multiplate reader (Promega, US) at a wavelength of 560 nm. The experimental sample concentrations were then extrapolated from the standard curve using the Microsoft Excel software.

2.2.3 Western Blotting Analysis

2.2.3.1 SDS-PAGE

The appropriate concentration of protein samples were separated by molecular weight using SDS-PAGE gels which were prepared as described in Section 2.1.6.1 above. All protein samples were prepared as shown in Table 2.1 below; heated to 95°C for 5 min to denature the protein and pulsed-spun briefly prior to loading onto the polyacrylamide gel.

Table 2.1: Components for protein sample preparation for SDS-PAGE.

Reagent	Volume (µl)
Protein sample (8,8 µg – 20 µg)*	x
100 mM DTT	1
5X SDS Loading Dye	6
1X RIPA Buffer	30-(x+7)
Total Volume	**30**

***Protein concentration varied to determine optimal detection of the protein for Western Blotting**

5 µl of the BenchMark™ Pre-stained 1 Kb Protein Ladder (Figure B1, Appendix B) was included in one of the lanes, and empty wells were loaded with 5 µl of 5X SDS loading dye (Appendix A) to ensure consistent protein movement along the gel. The gel was electrophoresed for 2-2.5 hours at 100 volts or as appropriate.

2.2.3.2 Protein Transfer onto Nitrocellulose Membrane

Once electrophesis was completed, the separated proteins were transferred to a Nitrocellulose membrane (Bio-Rad, California, USA). This was achieved by assembling the fiber pad, filter paper, polyacrylamide gel and nitrocellulose membrane in the correct order, as shown below in Figure 2.1, in a gel holder cassette. The cassette was then placed into the Mini-PROTEAN 3 casting apparatus (Bio-Rad, California, US), with cold 1X Transfer buffer (Appendix A) and an ice pack. The power pack was then set at 100 V for 75 minutes.

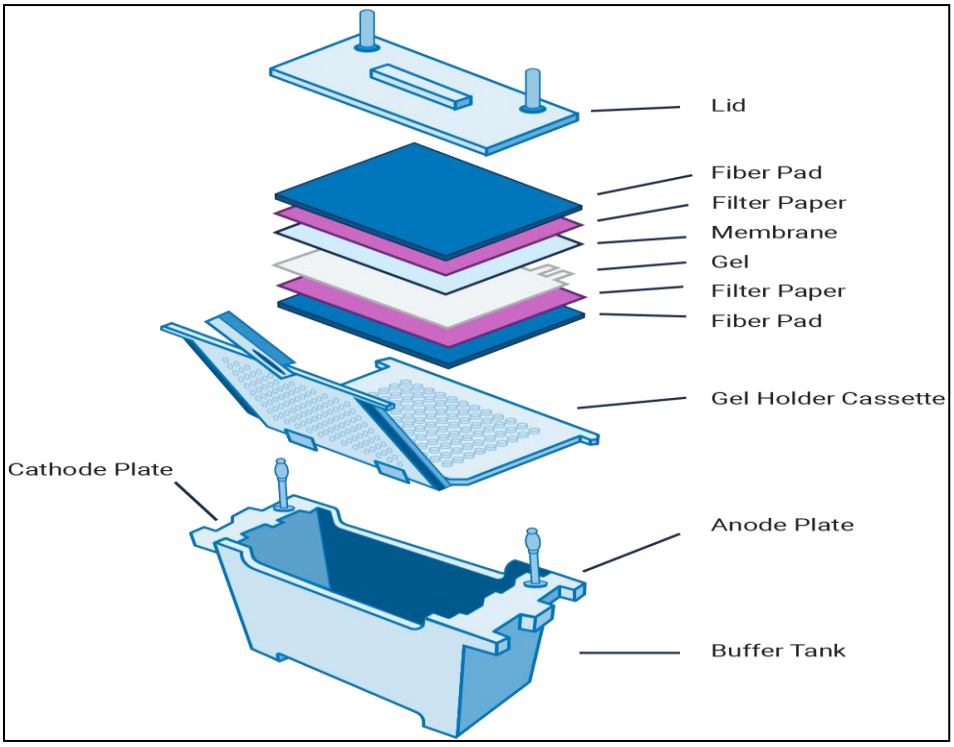

Figure 2.1: Diagram illustrating the "Western Blot Sandwich" cassette orientation for protein transfer. Adapted from: https://www.licor.com/bio/guide/westerns/transfer_options

2.2.3.3 Antibody Incubation and Protein Visualisation

Once the transfer was completed, the membrane was washed in 1XPBS containing 0,1% Tween-20 (PBST) (Appendix A) and thereafter stained with Ponceau S (Sigma Aldrich, Missouri, USA) (Appendix A) to confirm successful transfer. The stain was washed off using deionised water. The membrane was blocked in Blocking buffer (PBST containing 5% Fat-free milk) (Appendix A) for one hour at RT with gentle agitation, followed by incubation in primary antibody diluted in blocking buffer at 4°C, with gentle agitation, overnight. The primary antibodies used are Nef (NIH AIDS Research and Reference Reagent Program, USA; Catalog No. 2949); Cyclin A (Cell Signalling Technology, USA; Product No. 4656) Cyclin B1 (Cell Signalling Technology, USA; Product No. 12231); Cyclin E2 (Cell Signalling Technology, USA; Product No. 4131) and p38 (Sigma Aldrich, USA; Product No. M0800). The dilutions of both primary and secondary antibodies are shown in Table 2.2 below.

Table 2.2: Primary and Secondary Antibody dilutions used for Western Blot analysis

Protein	Primary Antibody	Secondary Antibody
Nef	1:1000 (Rabbit)	1:5000 (Goat Anti-Rabbit)
Cyclin A	1:1000 (Mouse)	1:5000 (Horse Anti-Mouse)
Cyclin B1	1:1000 (Rabbit)	1:5000 (Goat Anti-Rabbit)
Cyclin E2	1:1000 (Rabbit)	1:5000 (Goat Anti-Rabbit)
p38	1:5000 (Rabbit)	1:5000 (Goat Anti-Rabbit)

After overnight incubation, the membrane was washed with PBST (2 X 5 minutes followed by 2 X 10 minutes) with gentle agitation at RT, followed by incubation in the appropriate HRP-conjugated secondary antibody (Table 2.2), diluted in blocking buffer, for 1 hour at RT with gentle agitation. The membrane was washed as before and visualised by enhanced chemiluminescence using the Clarity™ Western ECL substrate as per the manufacturer's instructions (Bio-Rad, California, USA). Membranes were exposed to X-ray film and the resulting chemiluminescent signal captured by developing and fixing the film. Where quantification was required, the developed film of the western blot was scanned, and the intensity of the bands was quantified using the ImageJ software (National Institute of Health, Maryland, USA).

2.2.3.4 Membrane Stripping

For re-probing of nitrocellulose membranes, the antibodies were removed from the membrane by incubating in pre-heated stripping buffer (Appendix A) at 50°C for 30 minutes, with brief agitation every 10 minutes. Next, the membrane was washed twice for 10 minutes with PBST. The membrane was able to be reused from the blocking stage as described above. This procedure was employed when the membranes were probed for detection of an internal loading control protein (p38).

2.3 Cell Cycle Profiling using flow cytometry

Flow cytometric analysis was performed, using the BD FACSCalibur™ Flow Cytometer instrument (BD Biosciences, USA), to detect alterations to the cell cycle profile when cells were treated with recombinant Nef. Briefly, cells were

counted and plated in low-serum media approximately 16 hours prior to treatment. Cells were treated with recombinant Nef protein at a concentration of 400 ng/ml for 2, 4 and 6 hours or left untreated (control). All treatments were done in duplicates.

At the end of treatment, cells were counted, pelleted (1500 rpm; 5 min) and washed twice in 1 ml of 1XPBS. The cell suspension was then resuspended in 2 ml of 1XPBS and fixed by adding 5 ml of ice-cold 70% ethanol, drop-wise whilst simultaneously vortexing to prevent any clumping. Cells were then placed in -20°C freezer overnight. The following day the ethanol-fixed cells were centrifuged (1500 rpm; 5 min) and the ethanol was aspirated off. The cells were resuspended in 1 ml of 1XPBS and transferred to fresh 1,5 ml microcentrifuge tubes. Next, cells were then centrifuged at 6000 rpm for 1 min, and the pellet resuspended in 1 ml of 1XPBS. This step was repeated once more. The supernatant was carefully removed leaving approximately 50 µl of 1XPBS over the pellet. The cells were then resuspended in RNAse A (Stock: 10 mg/ml; Final concentration: 0,05 mg/ml) (Appendix A) diluted in 1X PBS, which was determined based on the number of cells. For example, if the number of cells counted was 60×10^4 cells in 10 ml of cell suspension, the volume of RNAase A solution added per sample will be 600 µl. Cells were then incubated in the PI staining solution (Appendix A) at 4°C overnight. Propidium Iodide (PI) is a fluorochrome known for binding to nuclear DNA, thus allowing it to be stained [98]. The volume of the PI staining solution used was nine times the volume of the RNAse A solution. The cell solution was then subject to flow cytometric analysis using the BD FACSCalibur™ Flow Cytometer instrument. The forward and side scatter, the DNA content and overall cell cycle profile was visualized using the BD Cell Quest Pro™ software (Version 5.2.1, BD Biosciences, USA).

2.4 Annexin V/7-AAD Analysis

Ramos cells were plated in low-serum medium as described above, and thereafter treated with recombinant Nef protein at a concentration of 400 ng/ml for 6 hours (based on the results of the Cell viability assay, Section

2.1.6.3) or left untreated. At the end of the 6 hour treatment, cells were exposed to Doxorubicin, at a final concentration of 0,35 µg/ml for 24 hours to induce apoptosis. The various treatment groups are outlined in Table 2.3 below. To evaluate apoptosis, the Annexin V/7-Amino-actinomycin (7-AAD) staining assay was performed using the PE Annexin V Apoptosis Detection Kit I (BD Biosciences, USA). Independent experiments were performed at least in triplicate.

Table 2.3: Various treatment groups (Ramos Cells)

Treatment Group	Treatment(s)
Nef and Doxorubicin	Recombinant Nef (400 ng/ml; 6hrs) + Doxorubicin (0,35 µg/ml; 24hrs)
Nef only	Recombinant Nef (400 ng/ml; 6hrs)
Doxorubicin only	Doxorubicin (0,35 µg/ml; 24hrs)
No Nef or Doxorubicin (Untreated/Control)	No treatments received
Compensation Control (5% DMSO – Annexin V and 7-AAD positive population)	Plated in low serum media supplemented with 5%DMSO
Compensation Control (Untreated, Annexin V and 7-AAD negative population)	No treatments received

At the end of the treatments, cells were pelleted by centrifugation (1500; 5 min), resuspended in 2 ml medium and counted using the Haemocytometer. The cells were then pelleted again and resuspended in the appropriate volume of 1X Annexin Binding Buffer (based on the cell concentrations) to ensure a final cell concentration of 1×10^6 cells/ml. 100 µl of each cell suspension was removed and added to 5 ml Falcon Round Bottom Test Tubes, resulting in a final concentration of 1×10^5 cells/ml in each tube. Each treatment group was stained with both 5 µl of PE Annexin V and 5 µl of 7-AAD. Three tubes of the 5% DMSO control group was prepared, with one tube being stained with PE Annexin V only; another tube being stained with 7-AAD only and the final tube being stained with both. Two tubes of the untreated, normal population was included, with one tube being stained with both PE Annexin V and 7-AAD and another tube being left unstained (no PE Annexin V or 7-AAD). All tubes

were gently vortexed to ensure mixing, covered in foil to protect from light, and allowed to incubate for 15 min at RT. After incubation, 400 µl of 1X Annexin Binding buffer was added to each tube and the samples were then analysed on the BD FACSCalibur™ Flow Cytometer instrument using the BD Cell Quest Pro™ software. All compensation controls were read first to allow for correct compensation and size determination, followed by the experimental samples.

2.5 Sub-cellular Fractionation

To determine if HIV-1 Nef is being internalized by Ramos cells after extracellular exposure, cell lysates underwent sub-Cellular Fractionation using the Subcellular Protein Fractionation Kit for Cultured cells (Thermo Fisher Scientific™, Massachusetts, USA). This process yielded five different sub-cellular protein extracts which include the Membrane; Cytoplasmic; Nuclear; Chromatin-bound Nuclear and Cytoskeletal proteins. Ramos cells were plated in low-serum medium as described previously and treated the following day with recombinant Nef protein at a concentration of 400 ng/ml for 3 hours (concentration and time point was chosen based on the results of the Cell viability assay, Section 2.1.6.3) or left untreated. After the treatment period, the various fractions were isolated as per the manufacturer's instructions. Briefly, cells were pelleted by centrifugation at 500 × *g* for 5 minutes and resuspended in ice-cold 1XPBS. 1-10 × 10^6 cells were transferred to a 1,5 ml microcentrifuge tube and centrifuged at 500 × *g* for 2-3 minutes, and thereafter the various factions were extracted sequentially, in a stepwise process involving five specific extraction buffers containing protease inhibitors, namely, Cytoplasmic (CEB); Membrane (MEB); Nuclear (NEB); Nuclear (NEB containing $CaCl_2$ and Micrococcal Nuclease) and Pellet (PEB). The CEB is first added to the cell pellet, resulting in selective membrane permeabilization and the release of the soluble cytoplasmic content (cytoplasmic extract). The MEB is added next to break down the plasma, mitochondrial and ER-Golgi membranes (membrane extract) but leaves the nuclear membrane intact. Centrifugation allows for the recovery of the intact

nuclei (pellet), after which the NEB is added to the pellet to produce the soluble nuclear extract. To release the chromatin-bound nuclear proteins, additional NEB containing $CaCl_2$ and Micrococcal Nuclease is added. Finally, the PEB is added to the remaining insoluble pellet, isolating the cytoskeletal proteins. The volume of the cell pellet dictates the volume of all the extraction buffers used, with the volume ratio of CEB:MEB:NEB:PEB reagents being maintained at 200:200:100:100 µl, respectively. After fractionation was completed, protein quantification was performed used the BCA assay as described in Section 2.2.2.

2.6 Statistical Analyses

The two-way Analysis of Variance (ANOVA) test and the Dunnett's multiple comparison test was performed to test statistical significance (p <0,05) using the GraphPad PRISM version 8 for Windows, GraphPad Software, San Diego California, USA.

Chapter 3

Results

3.1 BL cells extracellularly treated with recombinant Nef protein display enhanced proliferation.

3.1.1 Verification of the specificity and integrity of recombinant HIV-1 Nef protein.

In previous studies done within the laboratory, cell treatments were performed using a recombinant HIS-tagged HIV-1 Nef protein (pET-14b-Nef SF2), which was developed in the laboratory by a previous Masters student [29]. Subsequently, we acquired another recombinant HIV-1 Nef protein, which was purchased from the AIDS Research and Reference Reagent Program (ARRP), with the latter being used for the current study. It was imperative to perform some quality checks on this product prior to commencing any experimental work. First, the integrity and relative quantity of the recombinant protein were verified using SDS-PAGE (Section 2.1.6.1) and BCA assay (Section 2.2.2), and second, the specificity of the protein was verified using Western blotting (Section 2.2.3).

3.1.1.1 The ARRP-Nef protein is stable and specific, but less concentrated than indicated.

The ARRP-Nef was electrophoresed by SDS-PAGE and compared side-by-side with our in-house HIS-tagged HIV-1 Nef protein. Additionally, BSA protein standards, of known concentrations, were also included. The gel was stained with Coomassie to allow for visualization (Section 2.1.6.2).

As shown in Figure 3.1, one major band is observed in lane 5 representing the ARRP-Nef protein, corresponding to the reported size of the Nef protein (27 kDa) [38]. Although some smearing can be observed above and below the main band, the integrity of the protein seems largely preserved, as opposed to the pET-14b-Nef SF2 in-house recombinant Nef protein (lanes 6-8), which

show three major bands in each lane, indicated by the three red arrows. It is likely that the in-house Nef protein is unstable and the smaller two bands are degradation products of the main larger protein.

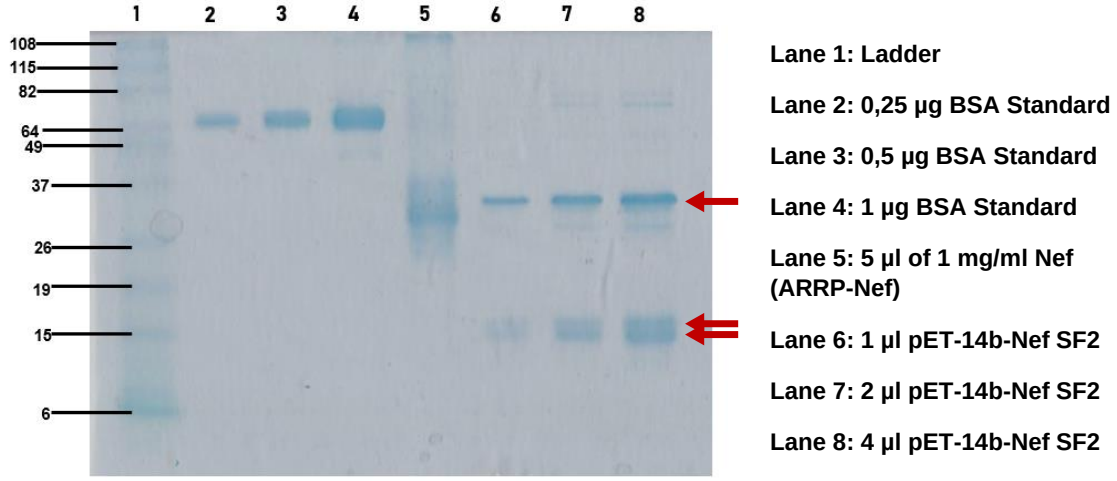

Figure 3.1: Recombinant HIV-1 Nef proteins on Coomassie stained SDS-PAGE gel. SDS-PAGE analysis followed by Coomassie staining of proteins as indicated for each lane. Lane 1 is the molecular weight marker. The red arrows indicate the three main bands of the in-house His-tagged Nef protein.

A second observation was that the intensity of the ARRP-Nef did not reflect the amount loaded (as per the concentration indicated on the stock tube – 1 mg/ml). A total of 5 µl of ARRP-Nef was loaded onto the gel, which should amount to 5 µg of protein. However, when compared to the BSA standards of known concentration (lanes 2-4), the band observed in lane 5 appeared to be of an intensity similar to that observed in lane 4, if not slightly less. To explore this further, BCA quantification was performed, using the BSA proteins as standards (Section 2.2.2). As is shown in the graph below (Figure 3.2), extrapolation based on the BSA standard curve produced a quantification amount of 0,55 mg/ml of ARRP-Nef, as opposed to the expected 1 mg/ml. This is approximately half of the expected stock concentration.

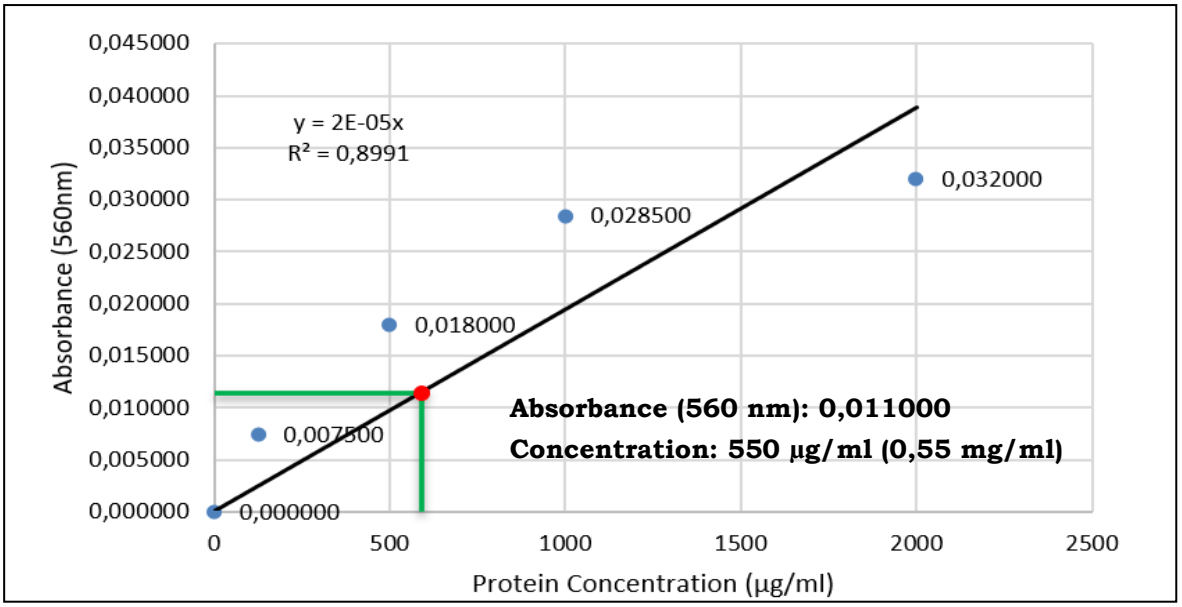

Figure 3.2: BSA Protein Standard Curve. Extrapolation using the standard curve indicated a concentration of 550 µg/ml (0,55 mg/ml). The red dot and green lines indicate the recorded absorbance and corresponding concentration of the ARRP-Nef protein (values are indicated on the graph).

To verify that the ARRP-Nef protein is indeed Nef, western blotting was performed (Section 2.2.3) using a Nef specific antibody. Based on the results of the BCA quantification assay performed above, 2 µg of both recombinant Nef proteins (ARRP and pET-14b-Nef SF2) were separated by SDS-PAGE and transferred onto a nitrocellulose membrane. As a positive control, 1 µl of cell lysate from HT1080 cells transfected with a Nef-expressing mammalian expression construct (Section 2.1.3) was also included. As can be seen in Figure 3.3, a major band representing the Nef protein (lane 2, black arrow) was clearly observed for the ARRP-Nef protein. In addition to this, there are higher molecular weight bands present in the same lane (displaying a lower intensity compared to the main band) which is assumed to be residual Nef protein that did not migrate fully, or a non-specific band, as it is not detected upon lower exposures (data not shown). For the in-house pET-14b-Nef SF2 recombinant protein, two main bands were detected (lane 1), corresponding to the regions where the three bands (representing the in-house Nef protein and its assumed degradation products) are located in the SDS-PAGE gels shown in Figure 3.1 (red arrows), as well as numerous higher molecular weight bands. This therefore confirms that the in-house Nef protein is much

more susceptible to degradation than the ARRP-Nef protein. The positive control (HT1080 cells expressing recombinant Nef protein) could be detected after longer exposure (Supplementary Figure B2, Appendix B). The ARRP-Nef protein was used for all future experiments, using the concentration 0,5 mg/ml, in accordance with the BCA assay.

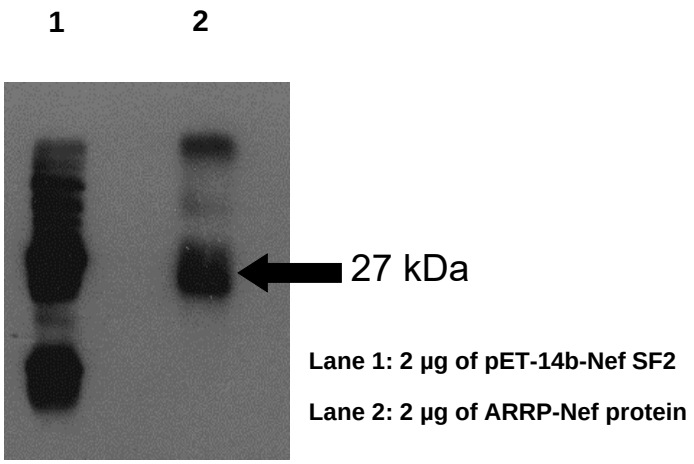

Figure 3.3: Western blotting analysis of recombinant Nef proteins (pET-14b-Nef SF2 and ARRP-Nef) using the polyclonal Nef antibody (NIH AIDS Research and Reference Reagent Program). The contents of each lane are indicated. The black arrow indicates the Nef protein (27kDa) of the ARRP-Nef.

3.1.2 Assessment of the effect of Nef on the cellular proliferation of BL cells.

As mentioned earlier in Chapter 1, Section 1.3.1.2, various studies have demonstrated that HIV-1 Nef is able to alter proliferation of certain cell types such as Non-Small Cell Lung Cancer (NSCLC) cells (cancerous epithelial cells), $CD4^+$ T cells and TF-1 cells, potentially enhancing tumorigenesis. A previous study in our laboratory has shown enhanced expression of the known pro-proliferative factor c-MYC, in BL cells that have been extracellularly exposed to Nef [52]. However, the corresponding phenotypic changes, including changes in proliferation, have not yet been explored, and therefore is one of the aims of this project.

3.1.2.1 Extracellular treatment with recombinant Nef protein leads to a 20% increase in cellular proliferation.

The two BL cells lines Ramos and BL-41 were plated in low serum medium approximately 16 hours prior to treatment. Serum starvation is a common technique employed in cell-based assays and is performed due to the

stimulatory effects of growth factors present within FBS that could potentially be concealing any cellular responses. Cells were treated extracellularly with ARRP-Nef at varying concentrations (0, 50; 100; 200 and 400 ng/ml) for 3; 6 and 24 hours (Section 2.1.5). These treatment conditions were selected based on previous studies done in our lab [52]. The WST-1 assay was performed as outlined in Section 2.1.6.3.

As shown in Figure 3.4A, for Ramos cells, a significant 20% increase in proliferation was measured for the highest concentration of 400 ng/ml ARRP-Nef, after an exposure time of 3 hours (dark grey bars). A small but reproducible increase, of approximately 10% in proliferation, was observed for 50 ng/ml ARRP-Nef treatment, with the highest increase noted at the longest exposure time of 24 hours (brown bars). For BL-41 cells (Figure 3.4B), a significant 20% increase in proliferation was measured for the highest concentration of 400 ng/ml ARRP-Nef, after an exposure time of 3 hours (dark grey bars), which is similar to what was observed for Ramos cells. Additionally, smaller increases in proliferation (~7-10%) were observed at an exposure time of 24 hours for 50, 100 and 200 ng/ml (brown, grey and light blue bars, respectively). These results demonstrated that recombinant Nef protein is able to cause an increase in proliferation in Ramos and BL-41 cells.

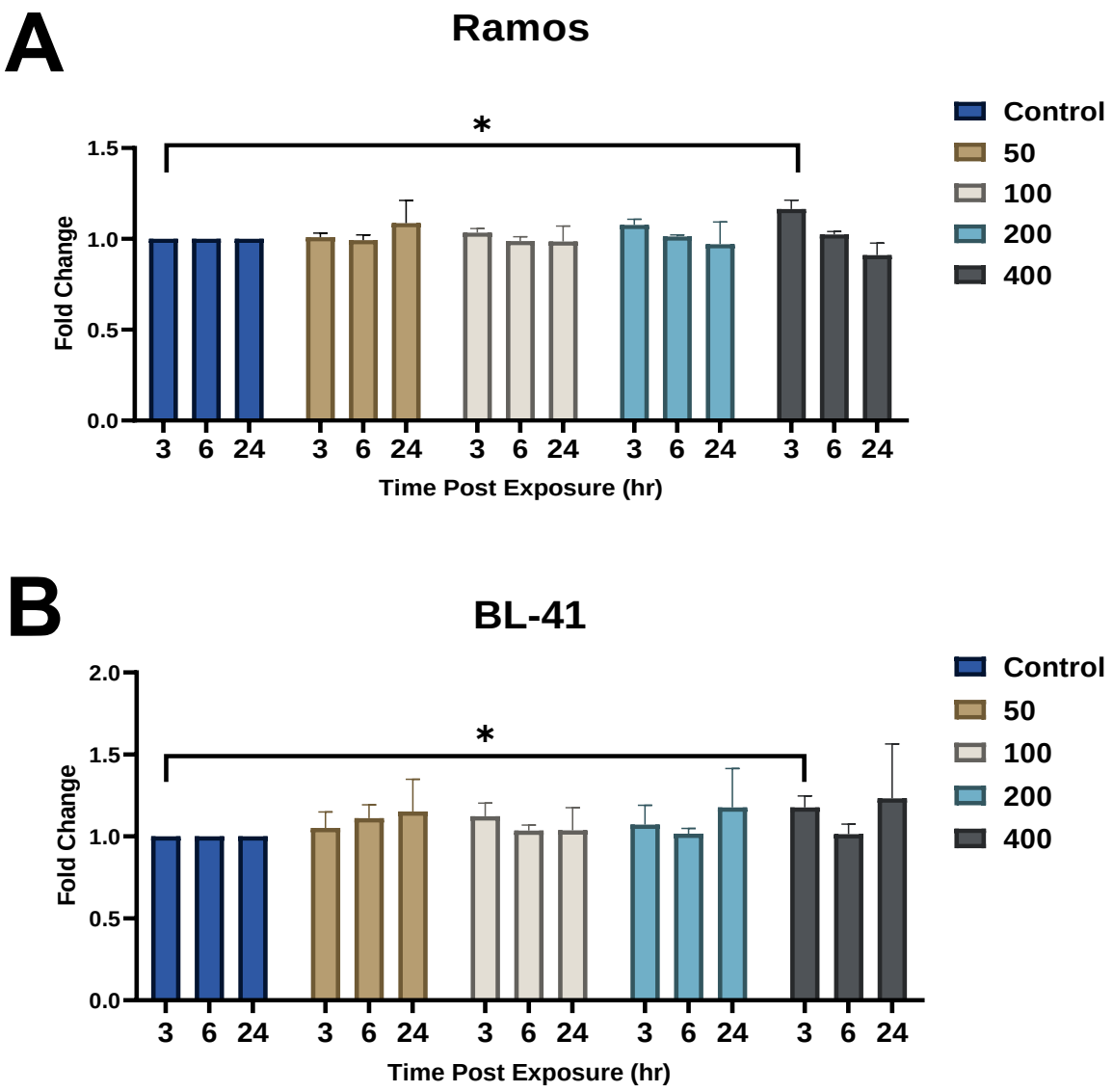

Figure 3.4: ARRP-Nef enhances cellular proliferation. Ramos (A) and BL-41 (B) cells were treated with recombinant Nef protein at varying concentrations (0; 50; 100; 200 and 400 ng/ml) for 3; 6 and 24 hours and thereafter proliferation was measured, relative to control (untreated cells) using the WST-1 cell proliferation reagent (Roche Applied Science, Penzberg, Germany). The colour coded bars indicate the different concentrations of protein used, and the exposure times are indicated on the x-axis. Error bars represent the standard deviation.* represents a *p*-value of ≤0,05 (a Two-way ANOVA test was performed using GraphPad PRISM 8, GraphPad Software, California, USA). Each experiment was performed at least in triplicate.

3.2 Investigation of the effect of Nef on expression of cell cycle proteins.

Cancer is characterized by uncontrollable tumour cell proliferation which is a direct result of aberrant activity of various cell cycle proteins. The progression of the cell cycle is governed by the presence of Cyclin-Dependent Kinases (CDKs) with their activation being dependent on the concentration of their corresponding cyclins [105]. CDKs are regulatory subunits that form complexes with their corresponding cyclin, acting specifically as checkpoint kinases of various target proteins involved in the regulation of cell cycle progression. For example, Cyclin D1 complexes with CDK4 and CDK6 to phosphorylate the retinoblastoma protein (pRB), resulting in the release of E2F from the pRB-E2F complex, allowing for the expression of various target genes related to proliferation [102, 103, 105]. The expression of cyclins are "cyclic", as their name implies, and continuously fluctuates during the cell cycle, and thus the expression of specific cyclins can be used to monitor cell proliferation [104, 105] (Figure 3.5).

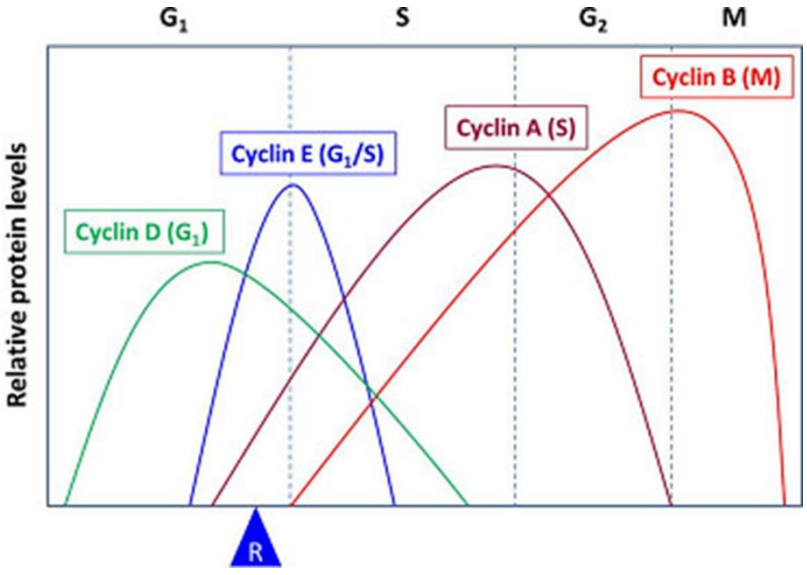

Figure 3.5: Cyclin expression levels throughout the four phases of the cell cycle. The class of each Cyclin is indicated by the letters in parenthesis. "R" represents the Restriction or G1 checkpoint. After passing this point, the cell will be fully committed to DNA synthesis [105, 112].

3.2.1 The expression of various cyclins are enhanced upon exposure to ARRP-Nef.

Results of the previous section (Section 3.1.2.1) indicated enhanced proliferation of BL cells in response to Nef protein exposure. Therefore, it would be interesting to see if the expression of certain cell cycle proteins

reflected the increase in proliferation that was observed. Thus, changes in the expression of specific cell cycle proteins was investigated in BL cells exposed to ARRP-Nef in comparison to controls. Ramos cells were plated as discussed before, and treated with 400 ng/ml of the recombinant viral protein, for two time points, an “early” timepoint of 3 hours, and a “late” timepoint of 24 hours. Thereafter, total soluble protein was harvested and used in western blot analyses (Section 2.2.3). As can be observed in Figure 3.6 below, an increase in expression of all three Cyclins was observed, but most notably for Cyclins B1 (20% increase at 24 hours) and E2 (60% increase at 24 hours). This indicated that exposure to ARRP-Nef did in fact enhance proliferation via the expression of cyclin proteins.

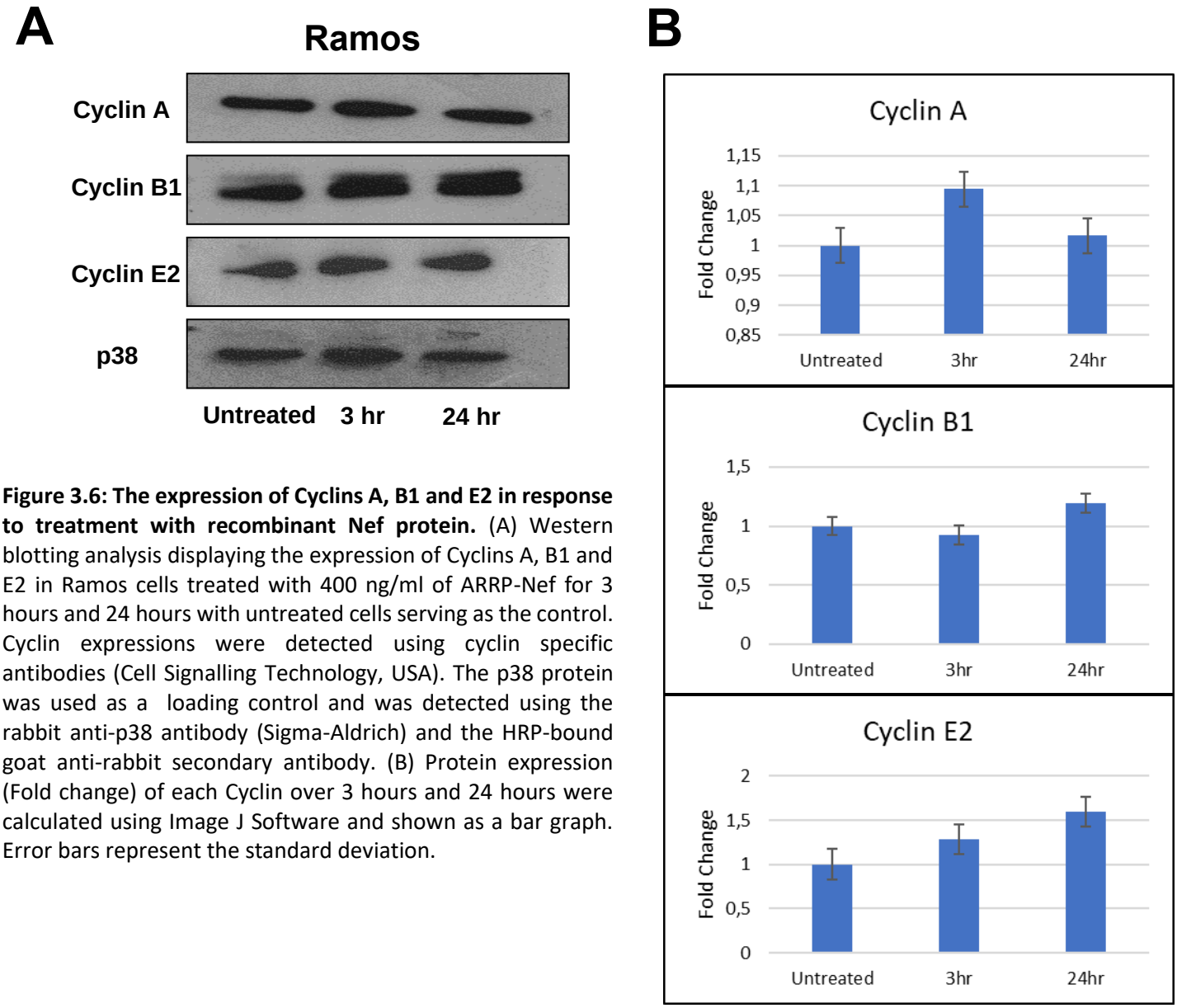

Figure 3.6: The expression of Cyclins A, B1 and E2 in response to treatment with recombinant Nef protein. (A) Western blotting analysis displaying the expression of Cyclins A, B1 and E2 in Ramos cells treated with 400 ng/ml of ARRP-Nef for 3 hours and 24 hours with untreated cells serving as the control. Cyclin expressions were detected using cyclin specific antibodies (Cell Signalling Technology, USA). The p38 protein was used as a loading control and was detected using the rabbit anti-p38 antibody (Sigma-Aldrich) and the HRP-bound goat anti-rabbit secondary antibody. (B) Protein expression (Fold change) of each Cyclin over 3 hours and 24 hours were calculated using Image J Software and shown as a bar graph. Error bars represent the standard deviation.

3.2.2 No major changes observed in cell cycle profile at early exposure, with enhanced sub-G1 peak at later exposure times.

Analysis of the cell cycle by DNA content is a method that is frequently employed to distinguish cells in different phases of the cell cycle, using flow cytometry. Changes in the typical profile of the cell cycle may provide clues on the mechanism of action of agents such as the Nef protein. Based on the above observations, we were interested in investigating the impact of Nef-exposure within the first 6 hours after exposure, and thus, Ramos cells were

treated with 400 ng/ml of ARRP-Nef for 2, 4 and 6 hours after which cells were processed for cell cycle profile analysis (Section 2.3). Control cells were left untreated.

Untreated Ramos cells display a normal cell cycle profile, with a majority of cells in the G1 phase of the cell cycle (~71%), followed by cells in the G2/M phase (~12%), with the remainder being in the S phase (~7%) (Figure 3.7; Table 3.1). It should be noted that a small sub-G1 peak (~10%) can be observed in the untreated sample, which may correspond to a natural apoptotic population. The results reveal that there were no major changes to the profile of Ramos cells exposed to 400 ng/ml Nef after 2 hours. Although there is a seemingly reduced sub-G1 peak at the 2 hour treatment point compared to untreated, the actual number of cells within that population represents only ~8% of the total population. At the later time points of 4 and 6 hours, significant increases in the sub-G1 peaks can be observed, corresponding to a ~33% and 30% increase respectively, with significant reductions in the other peaks. This indicates a potential increase in apoptosis upon exposure to Nef, which was unexpected (based on the previous results of this study).

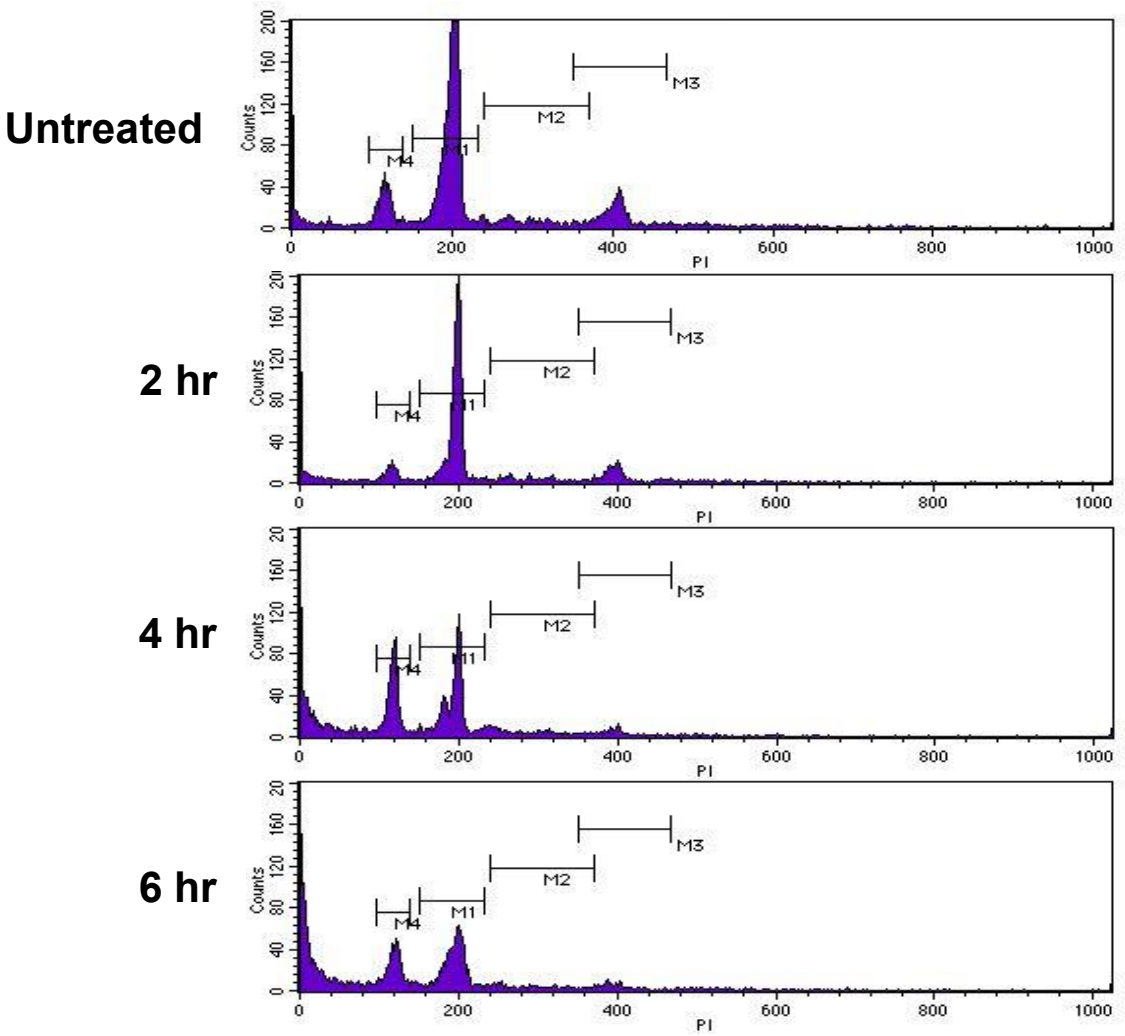

Figure 3.7: Cell cycle profiling of Ramos cells exposed to recombinant Nef protein. Ramos cells were treated with 400 ng/ml of ARRP-Nef protein for 2, 4 and 6 hours or left untreated (control). Cells were then stained with PI and processed for cell cycle profile analysis by flow cytometry. M1, M2, M3 represents the G0/G1, S, G2/M phases, respectively. M4 represents the Sub-G1 peak, which refers the population of cells with fragmented DNA. This experiment was perfromed at least in triplicates.

Table 3.1: The distribution of Ramos cells within different phases of the cell cycle in response to treatment with ARRP-Nef protein.

Treatment Groups				
	Untreated	**2 hours**	**4 hours**	**6 hours**
G0/G1 Peak	5110 (70, 86%)	2268 (71,21%)	1575 (49,10%)	1371 (51,74%)
S-Phase	524 (7,27%)	229 (7,19%)	334 (10,41%)	278 (10,49%)
G2/M Peak	845 (11,72%)	424 (13,31%)	233 (7,26%)	210 (7,92%)
Sub-G1 Peak	732 (10,15%)	264 (8,29%)	1066 (33,23%)	791 (29,85%)
Total Cell Count	7211	3185	3208	2650

3.3 Nef treatment does not induce apoptosis in B-cells, nor does it provide protection against cell death.

3.3.1 Nef does not induce apoptosis in B-cells.

The increase in the sub-G1 peaks observed at exposure times 4 and 6 hours in the assay described in Section 3.2 was perplexing because our earlier experiments indicated enhanced proliferation and expression of Cyclins A, B and E in response to treatment, which does not support a scenario of apoptosis. This warranted further investigation and therefore we next opted to use Annexin V/7-Amino-actinomycin (7-AAD) staining, a well-established technique that is used to measure apoptosis, and can allow for distinguishing between early apoptosis, late apoptosis and necrosis. When cells become apoptotic, the phospholipid component phosphatidylserine is exposed on the outer leaflet of the cell membrane. In the assay, Annexin V will bind to cells displaying this component as it has a high affinity for it. Annexin V is conjugated to a fluorochrome, allowing it to serve as a probe when flow cytometry is performed. 7-AAD is a DNA intercalating dye that can penetrate cells and bind to DNA only when membrane integrity is compromised (during late apoptosis and necrosis). Therefore, any viable cells will not be stained at all (Annexin V^- ,7-AAD^-), early apoptotic cells will be stained with Annexin V only (Annexin V^+, 7-AAD^-) and finally late apoptotic and necrotic cells will be stained by both (Annexin V^+, 7-AAD^+) [113].

Ramos cells were plated in low serum medium as previously described (Section 3.1.2.1), and then exposed to 400 ng/ml of ARRP-Nef for 6 hours. This time point was chosen as this was the latest time point used in the experiment described in Section 3.2.2 above, where a significant sub-G1 peak was observed. After treatment, cells were stained with Annexin V and 7-AAD and prepared for flow cytometric analysis as described in Section 2.4. Control cells were left untreated.

As can be seen in Figure 3.8 below, and contrary to what was observed in Figure 3.7 above, no significant increase in the percentage of cells positive for Annexin V, or 7AAD, or both, was observed after 6 hours of exposure to

recombinant Nef. A small percentage of Annexin V positive cells (5-6%) was found to naturally occur within the untreated Ramos population, and this was also the observation made for the untreated population shown in Figure 3.7. The result shown here was reproducible when the experiment was repeated (at least in triplicate).

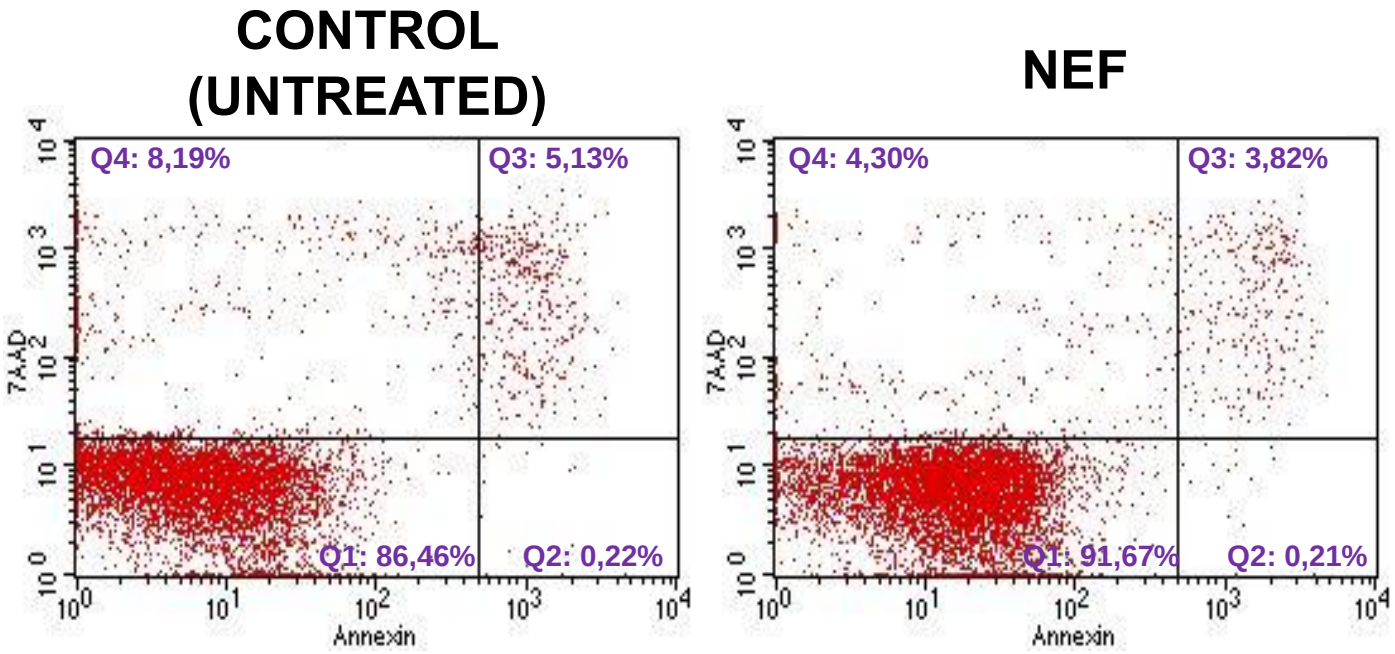

Figure 3.8: Annexin V/7-AAD staining using flow cytometry to evaluate Ramos cell apoptosis upon exposure to ARRP-Nef protein. Q1 refers to viable cells (Annexin V^- , 7-AAD^-); Q2 refers to early apoptotic cells (Annexin V^+, 7-AAD^-); Q3 and Q4 refers to late apoptotic and necrotic cells, respectively (Annexin V^+, 7-AAD^+). Labelling on top of each dot plot indicates the treatments received by the population. This experiment was performed at least in triplicates.

3.3.2 Nef does not protect against Doxorubicin-induced cell death in B-cells.

Having demonstrated that Nef provides a proliferative advantage to lymphoma cells, the next experiment was designed to investigate whether this viral protein provides a protective effect against cell death induced by chemotherapeutic agents. This is especially relevant in the context of the inferior response to chemotherapeutic treatment observed among HIV positive patients with aggressive lymphoma, compared to their HIV negative counterpart [124, 125]. Doxorubicin is a critical anti-cancer drug used in chemotherapeutic regimens for various cancers including Burkitt lymphoma, leukaemia, ovarian and lung cancer. Furthermore, Doxorubicin induces cell

death by intercalating DNA, resulting in the inhibition of DNA replication [114, 115].

In order to assess whether Nef could provide a protective effect against apoptosis, Ramos cells were exposed to ARRP-Nef (400 ng/ml) for 6 hours, after which Doxorubicin was added to the culture medium at a concentration of 0,35 µg/ml for 24 hours. This concentration was chosen based on previous observations made by our research group in which ~50% of cell death was observed when cells were treated with Doxorubicin (0,35 µg/ml) for 24 hours. Following Doxorubicin exposure, apoptosis was measured using the Annexin V assay, as outlined in Section 2.4. Controls included cells which were not pre-exposed to Nef, but did receive the Doxorubicin treatment, as well as cells which were left completely untreated. The results show that, while treatment with Doxorubicin led to almost the entire population becoming positive for Annexin V, the presence of the Nef protein caused no change to the level of apoptosis induced by Doxorubicin. This is evident by the lack of major changes observed in the various cell populations of cells exposed to Doxorubicin only, compared to cells exposed to Nef and Doxorubicin (Figure 3.9; upper and lower right quadrants). This therefore indicates that Nef did not provide any protective effect against Doxorubicin-induced cell death of Ramos cells. It is also important to note that the percentage of cells positive for Annexin V, when treated with 0,35 µg/ml for 24 hours was much higher than expected.

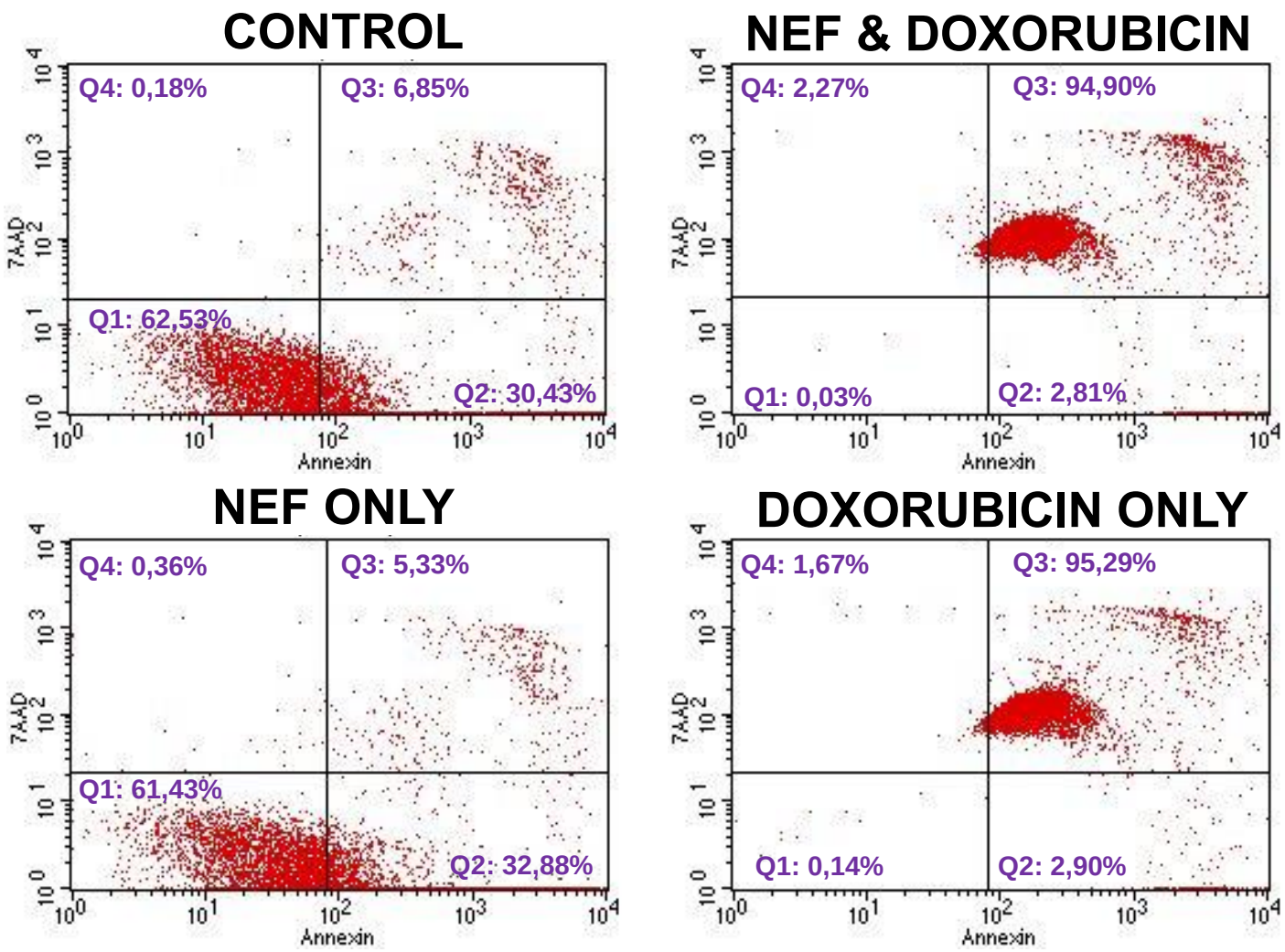

Figure 3.9: Annexin V/7-AAD staining using flow cytometry to evaluate the effect of the Nef protein on Doxorubicin-induced cell death in Ramos cells. Q1 refers to viable cells (Annexin V^- , 7-AAD^-); Q2 refers to early apoptotic cells (Annexin V^+, 7-AAD^-); Q3 and Q4 refers to late apoptotic and necrotic cells, respectively (Annexin V^+, 7-AAD^+). Labelling on top of each dot plot indicates the treatments received by the population. This experiment was done in at least triplicates.

3.4 Investigating the internalization of recombinant Nef protein in B-cells post extracellular exposure.

While only cells which harbour the CD4 receptor are known to be hosts for the HIV virus, several studies have found that HIV auxiliary proteins can invade other cell types. For instance, a study done by Xu *et al.* (which was briefly mentioned in Chapter 1, Section 1.3.1.2) used immunocytochemistry and flow cytometry to validate the presence and accumulation of the Nef protein in B-cells co-cultured with HIV-infected macrophages for 24 hours. The study reported that during HIV infection, Nef was shown to be trafficked to B-cells via specific conduits, formed by infected macrophages, which selectively attach to neighbouring B-cells [37]. Other studies have shown that the HIV p17 protein has the ability to bind the CXCR1/2 receptors on B cells and become internalized [33]. In an attempt to shed some clarity on the movement dynamics of ARRP-Nef within our experimental setting, an experiment was devised where cells were exposed to the protein and thereafter proteins were extracted from various cellular fractions and assessed for the presence of Nef using western blotting.

3.4.1 Successful cellular fractionation, protein extraction and transfer.

Ramos cells were treated with 400 ng/ml recombinant Nef protein for 3 hours. Control cells were left untreated. Sub-cellular fractionation was performed on cells, allowing for the extraction of protein from five different cellular components (sub-cellular protein extracts) (Figure 3.10), which consisted of the Membrane extract (ME), Cytoplasmic extract (CE), Nuclear extract (NE), Chromatin-bound Nuclear extract (CNE) and the Cytoskeletal extract (CSKE) (see Section 2.5 for detailed protocol).

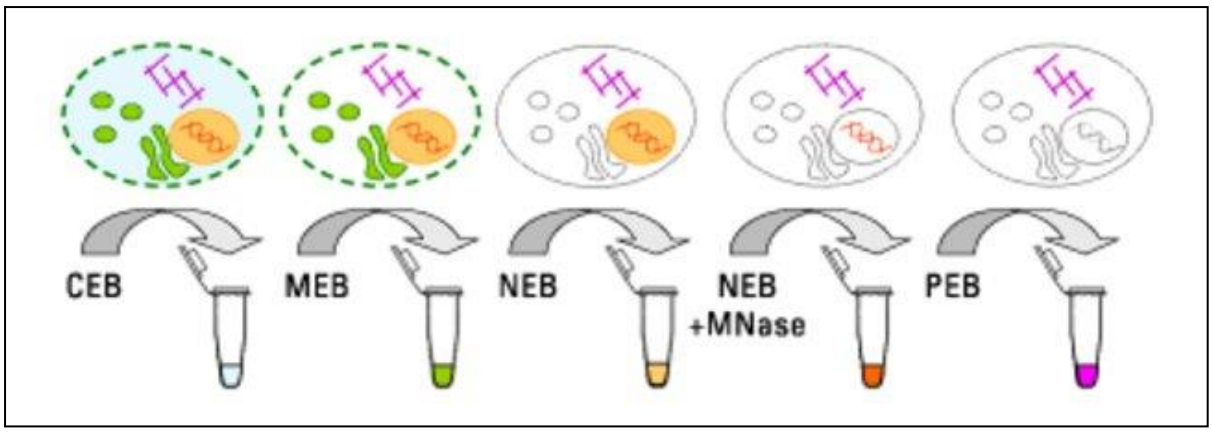

Figure 3.10: Diagram displaying an overview of the sub-cellular fractionation procedure. Various cellular components were extracted using extraction buffers: Cytoplasmic extraction buffer (CEB) followed by Membrane extraction buffer (MEB) and Nuclear extraction buffer (NEB). Micrococcal nuclease (MNase) was further added to NEB to separate chromatin-bound proteins from the cell pellet. Finally, the Pellet extraction buffer (PEB) was added to remove and solubilize cytoskeletal proteins. (Adapted from https://www.thermofisher.com/).

Protein isolates were quantified using the BCA assay (Section 2.2.2), separated using SDS-PAGE (Section 2.2.3.1) and transferred onto a nitrocellulose membrane (Section 2.2.3.2). In order to visualize the protein fractions, the membrane was stained with Ponceau S staining solution (Appendix A) as described in Section 2.2.3.3. The pattern of each protein fraction is distinct, as can be seen in Figure 3.11 below, and no major differences can be observed between the untreated (UT) and Nef-treated (T) lanes.

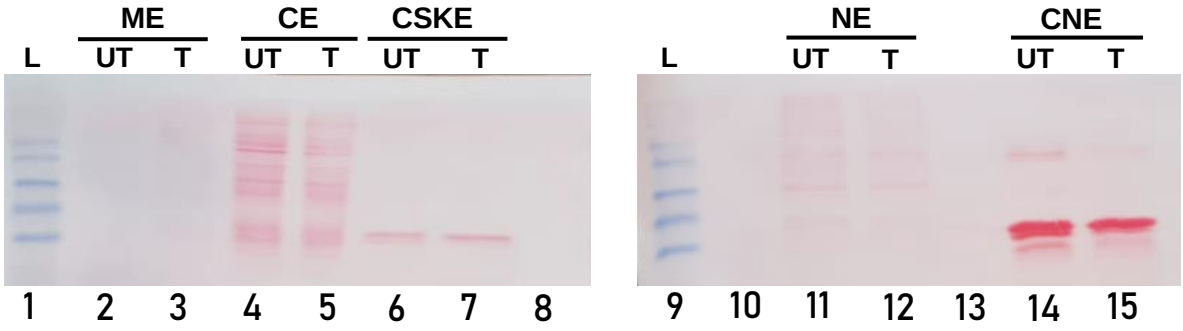

Figure 3.11: Ponceau S staining of blotted proteins of the different sub-cellular protein isolates (extracts). Ramos cells were treated with ARRP-Nef protein (400 ng/ml) for 3 hours (T) or left untreated (UT). Cells underwent sub-cellular fractionation to yield five protein extracts: Membrane extract (ME), Cytoplasmic extract (CE), Nuclear extract (NE), Chromatin-bound Nuclear extract (CNE) and Cytoskeletal extract (CSKE). Sub-cellular protein isolates were separated using SDS-PAGE, transferred onto nitrocellulose membranes and stained with Ponceau S. "L" denotes the BenchMark™ Pre-stained 1 Kb Protein Ladder (lanes 1 and 9).

3.4.2 Nef protein may localize to the cytoplasm and nucleus.

Next, western blotting analysis was performed, as briefly described in Section 2.2.3, on all protein extracts using a Nef-specific antibody to determine whether Nef could be detected in any of the extracts. This would allow us to determine if B-cells are internalizing Nef and if so, to what compartment of the cell is the Nef protein being localised to. As a positive control for the western blotting experiment, total cellular protein extracts from HT1080 cells transfected with a Nef expressing plasmid was used (Section 2.1.3).

As shown in Figure 3.12 below, numerous bands were detected within the positive control lanes (lanes 8 and 15) with the blue arrow pointing to what is assumed to be the band representing the Nef protein, based on size. Bands of a similar size to the positive control is seen in the Cytoplasmic (CE) (lanes 3 and 4) and Nuclear (NE) (lanes 9 and 10) extracts. However, these bands are also present in both the untreated (UT) and Nef-exposed lanes (T), which therefore means that they may not be “true” Nef protein bands. In the Cytoskeletal extract (CSKE), two bands of a higher molecular weight, compared to the CE, appear in both untreated and Nef-exposed lanes (lanes 5 and 6) and do not correspond with the Nef protein band of the positive control. No notable bands can be seen in the Membrane extract (ME) (lanes 1 and 2) or the Chromatin-bound Nuclear extract (CNE) (lanes 12 and 13) which indicates the likelihood that the amount of Nef protein present within these cellular fractions are very low. Several steps could be taken to improve on these results, which will be elaborated upon in the discussion section. Due to time constraints, a repeat could not be performed within the available timeframe.

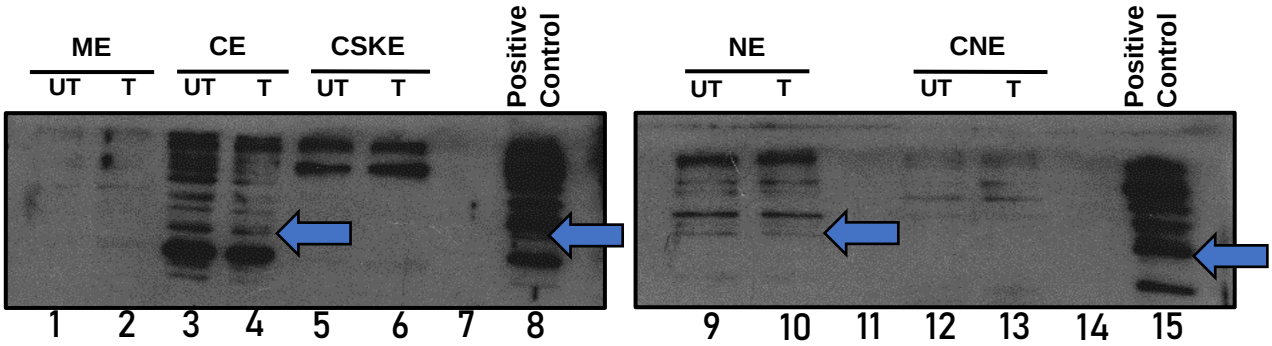

Figure 3.12: Western blotting analysis of the sub-cellular protein isolates (extracts) for the presence of the Nef protein. Ramos cells were treated with ARRP-Nef protein (400 ng/ml) for 3 hours (T) or left untreated (UT). Cells underwent sub-cellular fractionation to yield five protein extracts: Membrane extract (ME), Cytoplasmic extract (CE), Nuclear extract (NE), Chromatin-bound Nuclear extract (CNE) and Cytoskeletal extract (CSKE). The presence of the Nef protein was detected using an anti-Nef antibody (NIH AIDS Research and Reference Reagent Program). The blue arrows indicate where the Nef protein is potentially located. The Positive control represents total cellular protein extract from HT1080 cells transfected with a Nef expressing plasmid.

Chapter 4

Discussion and Conclusion

As mentioned in the literature review (Chapter 1), HIV-associated cancers such as Burkitt lymphoma (BL) are overrepresented within the HIV infected population. Initially, the high incidence of such cancers was attributed to the immunosuppressive role of HIV. However, recent studies have shown that HIV-1 viral proteins are capable of directly driving oncogenic processes. These viral proteins have been shown to either act alone or in conjunction with cellular proteins and, in some cases, oncoproteins of certain oncogenic viruses such as the Kaposi's Sarcoma-associated Herpes Virus (KSHV) and the Epstein-Barr Virus (EBV). Prior studies have extensively reported on the potentially oncogenic capabilities of HIV-1 viral proteins such Tat, p17 and Nef [14-16, 19, 24, 25, 33, 34, 55]. However, of note to this study is the oncogenic function of HIV Nef protein in the development of BL.

A review of the literature reveals that the Nef protein plays a potentially oncogenic role in several cancer types. In Kaposi's Sarcoma (KS), Nef has been reported to synergize with viral oncoproteins of KSHV to enhance angiogenesis and tumorigenesis [25, 54]. In Non-Small Cell Lung Cancer (NSCLC), the presence of Nef resulted in a more aggressive phenotype by enhancing proliferation, angiogenesis and decreasing the expression of p53. Furthermore, Nef has also been shown to enhance proliferation in other cell types such $CD4^+$ T-cells and TF-1 cells [50, 72, 85]. Additionally, Nef has been linked to other cancer hallmarks including the inhibition of apoptosis and autophagy. In MOLT-4 cells (human leukaemia CD4-expressing T-cell line), the N-terminus of the Nef protein was shown to directly interfere with p53, resulting in the inhibition of p53-dependent apoptosis [90]. Nef has also been shown to disrupt the process of autophagy, potentially driving tumorigenesis as the dysregulation of autophagy has long been associated with cancer [48, 95]. These reports illustrate a clear oncogenic role for this viral protein.

There is currently little knowledge available on the oncogenic role of Nef in B-cells, and the possible contribution to lymphomagenesis. Previous work done by our research group shed some light on this matter and reported that Nef was able to increase the expression of two key lymphoma promoting factors (c-MYC and AID) and cause increased genomic instability, in BL cells. Genomic instability is a precursor of chromosomal translocations, a hallmark feature of haematopoietic malignancies including BL [52]. In this study, we set out to investigate the phenotypic changes associated with extracellular exposure of BL cells to the Nef protein, in order to further understand the oncogenic role of Nef in B-cell lymphoma. Since B cells are not hosts to HIV, the extracellular exposure mimics an *in vivo* scenario, where these lymphocytes are exposed to soluble viral proteins circulating in the serum of HIV infected patients. In the current study, following Nef-exposure, cells were monitored for changes in proliferation, expression of key cell cycle proteins (cyclins), the cell cycle profile, and the ability to provide protection against apoptosis. Additionally, a preliminary attempt was made to assess the potential internalization and trafficking of Nef within B cells.

The results of this study found that treatment with the Nef protein caused an increase in B-cell proliferation (Figure 3.4). An increase in proliferation was confirmed by increases in Cyclins A, B and E (Figure 3.6). Cell cycle profiling showed an increase in the sub-G1 peak at later exposure times in BL cells exposed to the Nef protein (Figure 3.7), indicating that apoptosis could be occurring, which was contrary to what was shown in the viability assays and with changes in the cyclin expression. However, using an apoptosis assay, this was found to be an anomaly, and no significant changes in apoptosis was confirmed to be taking place upon exposure to Nef (Figure 3.8). The findings of this project also indicate that Nef did not provide any protective effect against apoptosis induced by the chemotherapeutic agent Doxorubicin (Figure 3.9). Finally, the initial attempt to investigate potential internalization of Nef by B cells was inconclusive, and ways to improve on the experimental design is discussed below.

Our in-house recombinant Nef protein (pET-14b-Nef SF2) was less stable than the recombinant Nef protein obtained through the AIDS Research and Reference Reagent Program (ARRP-Nef), and this was illustrated by the significantly higher level of degradation observed, compared to the ARRP-Nef protein. However, the concentration of the ARRP-Nef protein, as measured by BCA assay, and as observed on SDS-PAGE gel, was about half of the indicated concentration. Although not quite evident in the same way as seen for the in-house Nef protein, this could be attributed to degradation, possibly due to repeated freezing and thawing. The latter has been shown to cause the denaturation of proteins in aqueous solutions by inducing certain stressors (such as recrystallization, changes to pH, crystallization of buffer solutes) [116]. Furthermore, the buffer solution the protein is resuspended in must be considered as certain buffers, during a low freezing rate (<1°C/min), will experience salt precipitation, resulting in a pH shift (acidification) which could also be contributing to protein degradation [116]. The in-house recombinant Nef protein, which experienced more degradation, was eluted in a His-elution buffer which contained a sodium phosphate buffer (pH-7,7) and sodium chloride [29]. The addition of sodium chloride to a sodium phosphate buffer encourages crystallization of Na_2HPO_4 during freezing, resulting in a drop in pH, contributing to protein denaturation [116]. The degradation of ARRP-Nef protein most likely occurred due to the same process, as the ARRP-Nef protein is resuspended in 1XPBS. Freezing of 1XPBS encourages the recrystallization of $Na_2HPO_4.12H_2O$, resulting in a pH shift (~4 units down) [117]. Alternatively, there could have been potential error in the original quantification of the ARRP-Nef protein, prior to its shipment to our laboratories.

As mentioned earlier in this Chapter, hyperproliferation is one of the many phenotypic changes caused by the Nef protein in various cell types. Our results appear to reflect this as recombinant Nef protein was able to cause a significant increase in cellular proliferation of Ramos and BL-41 cells, which was most notable when cells were exposed to 400 ng/ml of the recombinant viral protein, for 3 hours (Figure 3.4). Although this increase is relatively small (20%), it is significant and reproducible, and indicates that this viral protein can provide a growth advantage to tumour cells, potentially driving

tumorigenesis. This could be a reason behind the clinical observation that cancers in HIV infected individuals progress faster, when compared to HIV uninfected individuals, even those receiving ART [61]. The results observed mirror those of previous studies that have also investigated the effect of the Nef protein on proliferation, although in other cancer cell types. For instance, a previous study showed that Nef protein, expressed intercellularly using a plasmid, was able to cause an increase in proliferation of a macrophage precursor cell line through a cytokine independent mechanism [50]. Another study demonstrated that NSCLC cells ectopically expressing the Nef protein (generated using a Nef-expressing plasmid) caused enhanced proliferation [72]. Our future studies should focus on performing a second assay that measures proliferation, such as the Bromodeoxyuridine (BrdU) incorporation assay, to further confirm this finding. Furthermore, the mechanism by which recombinant Nef protein causes increased proliferation in B-cells must be explored. Our results suggest that this mechanism could be occurring via the enhanced expression of the cyclin proteins A, B and E (Figure 3.6). The possibility exists that Nef could be enhancing the activity of transcription factors which activate the promoters of the cyclin genes. HIV auxiliary proteins have been found to collaborate with cellular transcription factors in order to enhance oncogenic events. For example, HIV protein Tat has been shown to collaborate with the Activator Protein-1 (AP-1) transcription factors, leading to enhanced expression of c-MYC [110]. Another mechanism could be through binding to or mimicking cellular components. For instance, Nef has been shown to structurally mimic the β-catenin binding sites on endogenous β-catenin ligands, an important regulator of the Wnt1 pathway, a signalling pathway which plays a role in promoting proliferation [100, 101]. In β-cells, of the pancreatic islets, Wnt signalling was shown to enhance its proliferation by promoting the expression of Cyclin D2 (a crucial regulator of the β-cell cycle)[120]. In addition to this study, various other studies have demonstrated a potential link between Wnt signalling and cyclin expression [121, 122]. Therefore, in B-cells, the Nef protein could potentially be enhancing B-cell proliferation by using Wnt signalling to drive the expression of certain cyclins. In future experiments, the status of the Wnt pathway in Nef-exposed B cells

should be explored. At around 24 hours post exposure, the proliferative effect of Nef was lost. One likely explanation for this is that recombinant Nef protein could be subject to protein degradation, which is most likely accelerated at 37°C after 24 hours during incubation of the cells. A second explanation could be due to augmented proliferation of Ramos cells, being a cancer cell line of high proliferative potential, resulting in the Nef effect being diluted.

Cell cycle profiling of Ramos cells exposed to the Nef protein for 2 hours showed no changes in their profile, while exposure for later times revealed an increase in the sub-G1 peak, accompanied by a significant reduction in the cell populations of the G0/G1; S and G2/M phases, as well as an overall reduction in the total population of cells that was gated using the flow cytometer (Figure 3.7) (Table 3.1). This was not an expected result, as previous treatments under the same conditions yielded enhanced cell activity, as demonstrated by the WST-1 cell viability assays in two BL cell lines. This result was found to be anomalous. A possible explanation for the reduced number of cells positive for Propidium Iodide (PI) staining at later time points is that cells were not appropriately stained due to the low concentration of PI within the stain (Appendix A), which was most likely not sufficient enough to effectively stain the entire population of Ramos cells. Another likely explanation would be that since cells were permeabilized using Triton X-100 (Appendix A), this may have resulted in the leakage of DNA out of the cell causing a complete loss of DNA content while staining took place, which could explain the unexpected appearance of the sub-G1 peak Furthermore, the preparation steps leading to analysis included numerous cell pelleting steps, via centrifugation, and pellet resuspension, via vigorous pipetting. This is likely to have resulted in massive damage to the cell population. Suspension cells are known to be highly susceptible to these mechanical manipulations. Therefore, the sub-G1 peaks observed at the latter time points cannot be taken as a true reflection of apoptosis.

To address this contradiction in the results, we went on to investigate whether apoptosis was being induced in response to Nef protein exposure using Annexin V/7-Amino-actinomycin (7-AAD) staining. The results revealed that

Nef did not induce apoptosis in B-cells (Figure 3.8), confirming that the enhanced sub-G1 peak observed at later exposure times during the cell cycle profiling is an anomaly.

Previous studies have demonstrated the capability of Nef to block apoptosis [50, 90, 111]. In the present study, this was investigated by inducing apoptosis using the chemotherapeutic agent Doxorubicin. Our current results show that Nef does not provide protection to cells exposed to Doxorubicin (Figure 3.9). This result does not align with previous studies in which Nef is reported to block apoptosis, although these studies involved the use of other cell types such as T-cells [50, 90, 111]. It should however be noted that, in our experiment, we aimed to achieve moderate cell death in our population when inducing apoptosis. However, this was not the case as treatment with 0,35 mg/ml of Doxorubicin for 24 hours resulted in almost 100% Annexin V positivity. Therefore, if Nef were to have a subtle protective effect, this would have been missed. Previous work in the laboratory had identified the concentration of 0,35 mg/ml Doxorubicin to induce approximately ~50% cell death after 24 hours in Ramos cells. The increased cell death could have been due to the Ramos cells not being in a healthy state, or a miscalculation of the Doxorubicin working solution. In future experiments, this could be resolved by using freshly cultured Ramos cells and re-assessing the toxic effect of the Doxorubicin working solution. Another way to improve on this result could be to adjust the design of the assay. In the current assay, cells were first pre-treated with recombinant Nef protein for 6 hours prior to exposure to Doxorubicin. Therefore, the viability of the Nef protein could be compromised at the end of this 6 hour pre-exposure time, as well as any cellular events it may have initiated. In future experiments, the length of time of this pre-exposure could be shortened to between 1 and 3 hours. More repeats should also be performed, until a firm conclusion can be made about the protective effect of Nef.

In reviewing the literature, very little information was found on the question of whether HIV-1 Nef is able to enter B-cells from the extracellular space. One study did demonstrate that Nef could use extensions/conduits of HIV infected

macrophages, to be trafficked directly into B-cells (Figure 1.5) [37]. However, this is not applicable to our study as Nef can also exist as an extracellular protein in the sera of an HIV-infected patient [118], therefore we extracellularly exposed cells to recombinant Nef protein. It is currently unknown whether Nef, by itself, is able to penetrate B-cells. Although a possibility does exist that Nef might not be even entering the cell and mediates its effects using cell surface molecules as previous studies indicated that Nef is able to interact with cell surface molecules like CD4 and MHC-I [38-41], as well as interact with and form a complex with the T-cell receptor (TCR) to mediate downstream effects [99]. The results of our study were however rather inconclusive due to several reasons. Firstly, protein separation was not adequate, due to the length of the SDS-PAGE gel: a longer resolving gel will lead to better separation. This ineffective separation contributed to the non-specific binding as a lot of protein was concentrated within a small area. This also indicates that blocking stage was sub-optimal. Therefore, in future, separation over a longer SDS-PAGE gel is required, as well as optimization of the blocking step. Another significant drawback is that the positive control did not function as expected. It is seldom that only one specific band is detected for Nef in the positive control. Generally, at least one or two other non-specific bands are detected, usually at higher molecular weights. However, in this case, almost the entire lane contained numerous bands, which made it extremely difficult to locate the correct Nef band. Nevertheless, the most appropriate positive control band was selected, based on size. Another significant anomaly is that, in addition to being detected in the treated group (3 hours post exposure) of the Cytoplasmic and Nuclear extracts/fraction, the Nef protein also appeared to be present in the corresponding control groups (untreated) for both extracts (Figure 3.12). The protein appearing in both treatment groups therefore indicates that the observed band is non-specific and not the Nef protein. Alternatively, one could assume that an error was made during the cell treatment stage, or the cell harvesting stage, where both treated and untreated wells received Nef, or wells were erroneously merged during harvesting. Furthermore, cross contamination between untreated and treated groups could have potentially

occurred when samples were loaded onto a gel for SDS-PAGE (Section 2.2.3.1). However, if we consider the results, as they are, they do appear to fall in line, somewhat, with what we know about the localisation of the Nef protein in the cell. Prior studies have indicated that during HIV infection, majority of the Nef protein remains in the cytosol, although Nef has been shown to be localised to the cell membrane by utilizing its myristoylated N-terminal anchor domain to attach to the cytoplasmic leaflet of the cell membrane [90, 91, 107]. Furthermore, the Nef protein was also reported to localize within the nucleus and at the nuclear membrane [90]. One particular study demonstrated that in Nef-transfected Raji cells (another BL cell line) that have undergone sub-cellular fractionation, the Nef protein was almost entirely present in the cytoskeletal fraction, with only a small amount of Nef being detected in the membrane fraction and no Nef being present within the cytoplasmic fraction [119]. While we used recombinant Nef protein, the previously mentioned studies either transfected a Nef-expressing plasmid or electroporated recombinant Nef protein directly into cells. Therefore, there is a strong possibility that we may not be able to achieve detection of Nef using this assay design as the amount of Nef used is extremely small and dilute, and of this, an even smaller percentage would be transported within the cells. It must be mentioned that the experimental design could include appropriate controls to validate whether sub-cellular fractionation was successful. Western blotting could be used to probe for protein known to be present in a specific compartment of the cell even after fractionation has occurred, therefore allowing us to confirm the identification of each protein isolate/extract. This experiment could not be repeated or improved within this study due to time constraints. Future studies that further investigate Nef internalization must be performed, possibly using another technique to track the localization of the Nef protein post extracellular exposure such as immunocytochemistry or immunofluorescence using a fluorescently tagged Nef protein.

Other limitations of the current study need to be considered. For instance, the high cell death achieved during Doxorubicin treatment of Ramos cells. As mentioned earlier, the concentration of Doxorubicin used (0,35 µg/ml)

resulted in almost 100% of the population becoming apoptotic, therefore if Nef was producing a subtle effect on apoptosis, it would most likely be missed.

Despite its limitations, this project did contribute new knowledge and allowed for a better understanding of the oncogenic role of HIV-1 protein Nef in the development of BL. Our data demonstrated that the Nef protein caused enhanced proliferation of cells, via enhanced expression of cyclin proteins. Therefore, this does shed some light on what phenotypical changes the Nef protein is able to cause that will potentially contribute to B-cell lymphomagenesis. In addition to optimizing and improving the experimental design of various assays used, future studies should focus on further defining the oncogenic potential of Nef by examining its role in processes/pathways known to be implicated in cancer, such as the various hallmarks of cancer in the context of B-cells and BL. These include processes such as cellular metastasis and invasion, autophagy, angiogenesis as well as the induction of oncogenic pathways such as the ERK/MAPK pathway or the AKT signalling pathway of which Nef has been shown to play a role in (Chapter 1, Section 1.3.1.2). In addition to this, determining the protein-protein interactions that Nef is a part of, as mentioned earlier, might also reveal how the Nef protein is able to potentially internalize itself into the cell. Ultimately, more research must be undertaken to further elucidate the oncogenic role of HIV-1 Nef protein in HIV-associated lymphomas such as BL.

Reference List

1. Herbst M. Fact sheet on cancer [Internet]. Cansa.org.za. 2017 [cited 23 January 2020]. Available from: https://www.cansa.org.za/files/2017/05/Fact-Sheet-Cancer-May-2017-1.pdf.
2. Sung H, Ferlay J, Siegel R, Laversanne M, Soerjomataram I, Jemal A et al. Global Cancer Statistics 2020: GLOBOCAN Estimates of Incidence and Mortality Worldwide for 36 Cancers in 185 Countries. CA: A Cancer Journal for Clinicians. 2021;71(3):209-249.
3. Jemal A, Bray F, Forman D, O'Brien M, Ferlay J, Center M et al. Cancer burden in Africa and opportunities for prevention. Cancer. 2012;118(18):4372-4384.
4. Moodley J, Walter F, Scott S, Mwaka A. Towards timely diagnosis of symptomatic breast and cervical cancer in South Africa. South African Medical Journal. 2018 [cited 23 January 2020];108(10):803.
5. Rebbeck T. Cancer in sub-Saharan. Science. 2020;367(6473):27-28.
6. [Internet]. Statssa.gov.za. 2021 [cited 30 September 2021]. Available from: http://www.statssa.gov.za/publications/P0302/P03022021.pdf
7. Dhokotera T, Bohlius J, Spoerri A, Egger M, Ncayiyana J, Olago V et al. The burden of cancers associated with HIV in the South African public health sector, 2004–2014: a record linkage study. Infectious Agents and Cancer. 2019;14(1).
8. Abayomi E, Somers A, Grewal R, Sissolak G, Bassa F, Maartens D et al. Impact of the HIV epidemic and Anti-Retroviral Treatment policy on lymphoma incidence and subtypes seen in the Western Cape of South Africa, 2002–2009: Preliminary findings of the Tygerberg Lymphoma Study Group. Transfusion and Apheresis Science. 2011;44(2):161-166.

9. Herbst M. Fact Sheet on AIDS-related Lymphoma [Internet]. Cansa.org.za. 2017 [cited 23 January 2020]. Available from: https://www.cansa.org.za/files/2017/11/Fact-Sheet-Aids-related-Lymphoma-NCR-2013-NA-web-Nov-2017.pdf.

10. Guiguet M, Boué F, Cadranel J, Lang J, Rosenthal E, Costagliola D. Effect of immunodeficiency, HIV viral load, and antiretroviral therapy on the risk of individual malignancies (FHDH-ANRS CO4): a prospective cohort study. The Lancet Oncology. 2009;10(12):1152-1159.

11. Xue M, Yao S, Hu M, Li W, Hao T, Zhou F et al. HIV-1 Nef and KSHV oncogene K1 synergistically promote angiogenesis by inducing cellular miR-718 to regulate the PTEN/AKT/mTOR signalling pathway. Nucleic Acids Research. 2014;42(15):9862-9879.

12. Torres H, Mulanovich V. Management of HIV Infection in Patients With Cancer Receiving Chemotherapy. Clinical Infectious Diseases.2014;59(1):106-114.

13. Yao S, Hu M, Hao T, Li W, Xue X, Xue M et al. MiRNA-891a-5p mediates HIV-1 Tat and KSHV Orf-K1 synergistic induction of angiogenesis by activating NF-κB signaling. Nucleic Acids Research. 2015;43(19):9362-9378.

14. Sall F, El Amine R, Markozashvili D, Tsfasman T, Oksenhendler E, Lipinski M et al. HIV-1 Tat protein induces aberrant activation of AICDA in human B-lymphocytes from peripheral blood. Journal of Cellular Physiology. 2019;:1-8.

15. El-Amine R, Germini D, Zakharova V, Tsfasman T, Sheval E, Louzada R et al. HIV-1 Tat protein induces DNA damage in human peripheral blood B-lymphocytes via mitochondrial ROS production. Redox Biology. 2018 ;15:97-108.

16. L. Lamers S, B. Fogel G, C. Huysentruyt L, S. McGrath M. HIV-1 Nef Protein Visits B-Cells via Macrophage Nanotubes: A Mechanism for

AIDS-Related Lymphoma Pathogenesis?. Current HIV Research. 2010;8(8):638-640.

17. Mapekula L, Ramorola B, Goolam Hoosen T, Mowla S. The interplay between viruses & host microRNAs in cancer – An emerging role for HIV in oncogenesis. Critical Reviews in Oncology/Hematology. 2019;137:108-114.

18. Herbst M. Fact Sheet on Burkitt Lymphoma [Internet]. Cansa.org.za. 2017 [cited 31 March 2019]. Available from: https://www.cansa.org.za/files/2017/11/Fact-Sheet-Burkitt-Lymphoma-NCR-2013-web-Nov-2017.pdf.

19. Phillips L, Opie J. The utility of bone marrow sampling in the diagnosis and staging of lymphoma in South Africa. International Journal of Laboratory Hematology. 2018;40(3):276-283.

20. Molyneux E, Rochford R, Griffin B, Newton R, Jackson G, Menon G et al. Burkitt's Lymphoma. The Lancet. 2012;379:1234-44.

21. Fujita S, Buziba N, Kumatori A, Senba M, Yamaguchi A, Toriyama K. Early Stage of Epstein-Barr Virus Lytic Infection Leading to the "Starry Sky" Pattern Formation in Endemic Burkitt Lymphoma. Archives for Pathology and Laboratory Medicine. 2004;128(5):549-552.

22. Martelli M, Ferreri A, Agostinelli C, Di Rocco A, Pfreundschuh M, Pileri S. Diffuse large B-cell lymphoma. Critical Reviews in Oncology/Hematology. 2013;87:146-171.

23. Davis R, Ngo VN, Lenz G, Pavel T, Young RM, Romesser PB et al. Chronic active B-cell-receptor signalling in diffuse large B-cell lymphoma. Nature. 2010;463:88-92.

24. Borges Á, Silverberg M, Wentworth D, Grulich A, Fätkenheuer G, Mitsuyasu R et al. Predicting risk of cancer during HIV infection. AIDS. 2013];27(9):1433-1441.

25. Xue M, Yao S, Hu M, Li W, Hao T, Zhou F et al. HIV-1 Nef and KSHV oncogene K1 synergistically promote angiogenesis by inducing cellular miR-718 to regulate the PTEN/AKT/mTOR signalling pathway. Nucleic Acids Research. 2014;42(15):9862-9879.

26. Yao S, Hu M, Hao T, Li W, Xue X, Xue M et al. MiRNA-891a-5p mediates HIV-1 Tat and KSHV Orf-K1 synergistic induction of angiogenesis by activating NF-κB signaling. Nucleic Acids Research. 2015;43(19):9362-9378.

27. De Falco G, Bellan C, Lazzi S, Claudio P, La Sala D, Cinti C et al. Interaction between HIV-1 Tat and pRb2/p130: a possible mechanism in the pathogenesis of AIDS-related neoplasms. Oncogene. 2003;22(40):6214-6219.

28. Lazzi S, Bellan C, De Falco G, Cinti C, Ferrari F, Nyongo A et al. Expression of RB2/p130 tumor-suppressor gene in AIDS-related non-Hodgkin's lymphomas: Implications for disease pathogenesis. Human Pathology. 2002;33(7):723-731.

29. Mdletshe N. The role of HIV proteins Tat and Nef in HIV/AIDS-related lymphoma: effects on c-MYC and AID expression [M.Sc. thesis]. Department of Clinical and Laboratory Sciences, Division of Haematology, University of Cape Town.; 2014.

30. Huang L, Li C, Pardee A. Human Immunodeficiency Virus Type 1 TAT Protein Activates B Lymphocytes. Biochemical and Biophysical Research Communications. 1997;237:461-464.

31. Kurnaeva M, Sheval E, Musinova Y, Vassetzky Y. Tat basic domain: A “Swiss army knife” of HIV-1 Tat?. Reviews in Medical Virology. 2019;29(2):e2031.

32. Germini D, Tsfasman T, Klibi M, El-Amine R, Pichugin A, Iarovaia O et al. HIV Tat induces a prolonged MYC relocalization next to IGH in circulating B-cells. Leukemia. 2017;31(11):2515-2522..

33. Martorelli D, Muraro E, Mastorci K, Dal Col J, Faè D, Furlan C et al. A natural HIV p17 protein variant up-regulates the LMP-1 EBV oncoprotein and promotes the growth of EBV-infected B-lymphocytes: Implications for EBV-driven lymphomagenesis in the HIV setting. International Journal of Cancer. 2015;137(6):1374-1385.

34. Caccuri F, Giagulli C, Bugatti A, Benetti A, Alessandri G, Ribatti D et al. HIV-1 matrix protein p17 promotes angiogenesis via chemokine receptors CXCR1 and CXCR2. Proceedings of the National Academy of Sciences. 2012;109(36):14580-14585.

35. Levy D, Refaeli Y, Weiner D. Extracellular Vpr protein increases cellular permissiveness to human immunodeficiency virus replication and reactivates virus from latency. Journal of virology. 1995;69(2):1243-1252.

36. Ferrucci A, Nonnemacher M, Cohen É, Wigdahl B. Extracellular human immunodeficiency virus type 1 viral protein R causes reductions in astrocytic ATP and glutathione levels compromising the antioxidant reservoir. Virus Research. 2012;167(2):358-369.

37. Xu W, Santini P, Sullivan J, He B, Shan M, Ball S et al. HIV-1 evades virus-specific IgG2 and IgA responses by targeting systemic and intestinal B cells via long-range intercellular conduits. Nature Immunology. 2009;10(9):1008-1017.

38. Basmaciogullari S, Pizzato M. The activity of Nef on HIV-1 infectivity. Frontiers in Microbiology. 2014;5:1-7.

39. Pereira E, daSilva L. HIV-1 Nef: Taking Control of Protein Trafficking. Traffic. 2016;17(9):976-996..

40. Ding S, Gasser R, Gendron-Lepage G, Medjahed H, Tolbert W, Sodroski J et al. CD4 Incorporation into HIV-1 Viral Particles Exposes Envelope Epitopes Recognized by CD4-induced Antibodies. Journal of Virology. 2019;.

41. Peng B, Robert-Guroff M. Deletion of N-terminal myristoylation site of HIV Nef abrogates both MHC-1 and CD4 down-regulation. Immunology Letters. 2001;78(3):195-200.

42. Schwartz O, Maréchal V, Gall S, Lemonnier F, Heard J. Endocytosis of major histocompatibility complex class I molecules is induced by the HIV–1 Nef protein. Nature Medicine. 1996;2(3):338-342.

43. Zeller K, Zhao X, Lee C, Chiu K, Yao F, Yustein J et al. Global mapping of c-Myc binding sites and target gene networks in human B cells. Proceedings of the National Academy of Sciences. 2006;103(47):17834-17839.

44. Varin A, Manna S, Quivy V, Decrion A, Van Lint C, Herbein G et al. Exogenous Nef Protein Activates NF-κB, AP-1, and c-Jun N-Terminal Kinase and Stimulates HIV Transcription in Promonocytic Cells. Journal of Biological Chemistry. 2002;278(4):2219-2227.

45. Schrager J, Der Minassian V, Marsh J. HIV Nef Increases T Cell ERK MAP Kinase Activity. Journal of Biological Chemistry. 2001;277(8):6137-6142.

46. Fujinaga K, Zhong Q, Nakaya T, Kameoka M, Meguro T, Yamada K et al. Extracellular Nef Protein Regulates Productive HIV-1 Infection from Latency. The Journal of Immunology. 1995;155:5289-5298.

47. Lenassi M, Cagney G, Liao M, Vaupotič T, Bartholomeeusen K, Cheng Y et al. HIV Nef is Secreted in Exosomes and Triggers Apoptosis in Bystander CD4+ T Cells. Traffic. 2009;11(1):110-122.

48. Saribas A, Khalili K, Sariyer I. Dysregulation of autophagy by HIV-1 Nef in human astrocytes. Cell Cycle. 2015;14(18):2899-2904.

49. Brigino E, Haraguchi S, Koutsonikolis A, Cianciolo G, Owens U, Good R et al. Interleukin 10 is induced by recombinant HIV-1 Nef protein involving the calcium/calmodulin-dependent phosphodiesterase signal transduction pathway. Proceedings of the National Academy of Sciences. 1997;94(7):3178-3182.

50. Choi H, Smithgall T. HIV-1 Nef Promotes Survival of TF-1 Macrophages by Inducing Bcl-XL Expression in an Extracellular Signal-regulated Kinase-dependent Manner. Journal of Biological Chemistry. 2004;279(49):51688-51696.

51. Mangino G, Famiglietti M, Capone C, Veroni C, Percario Z, Leone S et al. HIV-1 Myristoylated Nef Treatment of Murine Microglial Cells Activates Inducible Nitric Oxide Synthase, NO2 Production and Neurotoxic Activity. PLOS ONE. 2015;10(6):e0130189.

52. Mdletshe N, Nel A, Shires K, Mowla S. HIV Nef enhances the expression of oncogenic c-MYC and activation-induced cytidine deaminase in Burkitt lymphoma cells, promoting genomic instability. Infectious Agents and Cancer. 2020;15(1)..

53. Wang Y, Li D, Fan H, Tian L, Zhong Y, Zhang Y et al. Cellular Uptake of Exogenous Human PDCD5 Protein. Journal of Biological Chemistry. 2006;281(34):24803-24817.

54. Zhu X, Guo Y, Yao S, Yan Q, Xue M, Hao T et al. Synergy between Kaposi's sarcoma-associated herpesvirus (KSHV) vIL-6 and HIV-1 Nef protein in promotion of angiogenesis and oncogenesis: role of the AKT signaling pathway. Oncogene. 2013;33(15):1986-1996.

55. Yang W, Lin T, Chang L, Yeh W, Huang S, Chen T et al. HIV-1 Tat Interacts with a Kaposi's Sarcoma-Associated Herpesvirus Reactivation-Upregulated Antiangiogenic Long Noncoding RNA, LINC00313, and Antagonizes Its Function. Journal of Virology. 2019;94(3).

56. Testoni M, Zucca E, Young K, Bertoni F. Genetic lesions in diffuse large B-cell lymphomas. Annals of Oncology. 2015;26(6):1069-1080.

57. Sehn L, Gascoyne R. Diffuse large B-cell lymphoma: optimizing outcome in the context of clinical and biologic heterogeneity. Blood. 2015;125(1):22-32.

58. Chapuy B, Stewart C, Dunford AJ, Kim J, Kamburov A, Redd RA et al. Molecular subtypes of diffuse large B cell lymphoma are associated with distinct pathogenic mechanisms and outcomes. Nature. 2018;24:679-690.

59. Martinez-Martin N, Maldonado P, Gasparrini F, Frederico B, Aggarwal S, Gaya M et al. A switch from canonical to noncanonical autophagy shapes B cell responses. Science. 2017;355(6325):641-647.

60. Raney A, Shaw A, Foster J, Garcia J. Structural constraints on human immunodeficiency virus type 1 Nef function. Virology. 2007;368(1):7-16.

61. Nasi M, De Biasi S, Gibellini L, Bianchini E, Pecorini S, Bacca V et al. Ageing and inflammation in patients with HIV infection. Clinical & Experimental Immunology. 2016;187(1):44-52.

62. Ahmed R. Investigating the contribution of HIV Nef in HIV-associated Lymphoma [Honours]. University of Cape Town; 2019.

63. Hanahan D, Weinberg R. Hallmarks of Cancer: The Next Generation. Cell. 2011;144(5):646-674.

64. White E, DiPaola R. The Double-Edged Sword of Autophagy Modulation in Cancer. Clinical Cancer Research. 2009;15(17):5308-5316.

65. Levine B, Kroemer G. Autophagy in the pathogenesis of disease. Cell. 2008;132:37-42.

66. Sinha S, Levine B. The autophagy effector Beclin 1: a novel BH3-only protein. Oncogene. 2008;27(S1):S137-S148.

67. Westendorp M, Frank R, Ochsenbauer C, Stricker K, Dhein J, Walczak H et al. Sensitization of T cells to CD95-mediated apoptosis by HIV-1 Tat and gp120. Nature. 1995;375(6531):497-500.

68. Giagulli C, Magiera A, Bugatti A, Caccuri F, Marsico S, Rusnati M et al. HIV-1 matrix protein p17 binds to the IL-8 receptor CXCR1 and shows IL-8–like chemokine activity on monocytes through Rho/ROCK activation. Blood. 2012;119(10):2274-2283.

69. Rudnicka D, Schwartz O. Intrusive HIV-1-infected cells. Nature Immunology. 2009;10(9):933-934.

70. Colombrino E, Rossi E, Ballon G, Terrin L, Indraccolo S, Chieco-Bianchi L et al. Human immunodeficiency virus type 1 Tat protein modulates cell cycle and apoptosis in Epstein–Barr virus-immortalized B cells. Experimental Cell Research. 2004;295(2):539-548.

71. Lacy S, Barrans S, Beer P, Painter D, Smith A, Roman E et al. Targeted sequencing in DLBCL, molecular subtypes, and outcomes: a Haematological Malignancy Research Network report. Blood. 2020;.

72. Santerre M, Chatila W, Wang Y, Mukerjee R, Sawaya B. HIV-1 Nef promotes cell proliferation and microRNA dysregulation in lung cells. Cell Cycle. 2019;18(2):130-142.

73. Lehmann M, Walter S, Ylisastigui L, Striebel F, Ovod V, Geyer M et al. Extracellular HIV-1 Nef increases migration of monocytes. Experimental Cell Research. 2006;312(18):3659-3668.

74. Mizushima N, Yoshimori T, Levine B. Methods in Mammalian Autophagy Research. Cell. 2010;140(3):313-326.

75. Wei Y, Pattingre S, Sinha S, Bassik M, Levine B. JNK1-Mediated Phosphorylation of Bcl-2 Regulates Starvation-Induced Autophagy. Molecular Cell. 2008;30(6):678-688.

76. Furuya N, Yu J, Byfield M, Pattingre S, Levine B. The Evolutionarily Conserved Domain of Beclin 1 is Required for Vps34 Binding, Autophagy, and Tumor Suppressor Function. Autophagy. 2005;1(1):46-52.

77. Peralta E, Edinger A. Ceramide-induced starvation triggers homeostatic autophagy. Autophagy. 2009;5(3):407-409.

78. Spender L, O'Brien D, Simpson D, Dutt D, Gregory C, Allday M et al. TGF-β induces apoptosis in human B cells by transcriptional regulation of BIK and BCL-XL. Cell Death & Differentiation. 2009;16(4):593-602.

79. Zhang W, Shi H, Zhang M. Maspin overexpression modulates tumor cell apoptosis through the regulation of Bcl-2 family proteins. BMC Cancer. 2005;5(1).

80. Nemoto S, Xiang J, Huang S, Lin A. Induction of Apoptosis by SB202190 through Inhibition of p38β Mitogen-activated Protein Kinase. Journal of Biological Chemistry. 1998;273(26):16415-16420.

81. McLaughlin D, Faller E, Sugden S, MacPherson P. Expression of the IL-7 Receptor Alpha-Chain Is Down Regulated on the Surface of CD4 T-Cells by the HIV-1 Tat Protein. PLoS ONE. 2014;9(10):e111193.

82. Bagashev A, Sawaya B. Roles and functions of HIV-1 Tat protein in the CNS: an overview. Virology Journal. 2013;10(1).

83. Lee J, Lee G. Rapamycin treatment inhibits CHO cell death in a serum-free suspension culture by autophagy induction. Biotechnology and Bioengineering. 2012;109(12):3093-3102.

84. Colombrino E, Rossi E, Ballon G, Terrin L, Indraccolo S, Chieco-Bianchi L et al. Human immunodeficiency virus type 1 Tat protein modulates cell cycle and apoptosis in Epstein–Barr virus-immortalized B cells. Experimental Cell Research. 2004;295(2):539-548.

85. St. Gelais C, Coleman C, Wang J, Wu L. HIV-1 Nef Enhances Dendritic Cell-Mediated Viral Transmission to CD4+ T Cells and Promotes T-Cell Activation. PLoS ONE. 2012;7(3):e34521.

86. Swingler S, Zhou J, Swingler C, Dauphin A, Greenough T, Jolicoeur P et al. Evidence for a Pathogenic Determinant in HIV-1 Nef Involved in B Cell Dysfunction in HIV/AIDS. Cell Host & Microbe. 2008;4(1):63-76.

87. Tsfasman T, Klibi M, Pichugin A, Lipinski M, Vassetzky Y. HIV: implication in Burkitt lymphoma. Biopolymers and Cell. 2012;28(4):285-287.

88. Gajanayaka N, O'Hara S, Konarski Y, Fernandes J, Muthumani K, Kozlowski M et al. HIV and HIV-Tat inhibit LPS-induced IL-27 production in human macrophages by distinct intracellular signaling pathways. Journal of Leukocyte Biology. 2017;102(3):925-939.

89. Caccuri F, Rueckert C, Giagulli C, Schulze K, Basta D, Zicari S et al. HIV-1 Matrix Protein p17 Promotes Lymphangiogenesis and Activates the Endothelin-1/Endothelin B Receptor Axis. Arteriosclerosis, Thrombosis, and Vascular Biology. 2014;34(4):846-856.

90. Greenway, A.L.; McPhee, D.A.; Allen, K.; Johnstone, R.; Holloway, G.; Mills, J.; Azad, A.; Sankovich, S.; Lambert, P. Human immunodeficiency virus type 1 Nef binds to tumor suppressor p53 and protects cells against p53-mediated apoptosis. J. Virol. 2002, 76, 2692–2702.

91. Das SR, Jameel S. Biology of the HIV Nef protein. Indian J Med Res. 2005 Apr 1;121(4):315-2.

92. Kashiwagi H, McDunn J, Goedegebuure P, Gaffney M, Chang K, Trinkaus K et al. TAT-Bim Induces Extensive Apoptosis in Cancer Cells. Annals of Surgical Oncology. 2007;14(5):1763-1771.

93. Ma X, Zheng W, Wei D, Ma Y, Wang T, Wang J et al. High-level expression, purification and pro-apoptosis activity of HIV-TAT-survivin (T34A) mutant to cancer cells in vitro. Journal of Biotechnology. 2006;123(3):367-378.

94. Kyei G, Dinkins C, Davis A, Roberts E, Singh S, Dong C et al. Autophagy pathway intersects with HIV-1 biosynthesis and regulates viral yields in macrophages. Journal of Cell Biology. 2009;186(2):255-268.

95. Castro-Gonzalez S, Shi Y, Colomer-Lluch M, Song Y, Mowery K, Almodovar S et al. HIV-1 Nef counteracts autophagy restriction by enhancing the association between BECN1 and its inhibitor BCL2 in a PRKN-dependent manner. Autophagy. 2020;17(2):553-577.

96. Kamiloglu S, Sari G, Ozdal T, Capanoglu E. Guidelines for cell viability assays. Food Frontiers. 2020;1(3):332-349.

97. Smith P, Krohn R, Hermanson G, Mallia A, Gartner F, Provenzano M et al. Measurement of protein using bicinchoninic acid. Analytical Biochemistry. 1985;150(1):76-85.

98. Riccardi C, Nicoletti I. Analysis of apoptosis by propidium iodide staining and flow cytometry. Nature Protocols. 2006;1(3):1458-1461.

99. Xu X, Laffert B, Screaton G, Kraft M, Wolf D, Kolanus W et al. Induction of Fas Ligand Expression by HIV Involves the Interaction of Nef with the

T Cell Receptor ζ Chain. Journal of Experimental Medicine. 1999;189(9):1489-1496.

100. Weiser K, Barton M, Gershoony D, DasGupta R, Cardozo T. HIV's Nef Interacts with β-Catenin of the Wnt Signaling Pathway in HEK293 Cells. PLoS ONE. 2013;8(10):e77865.

101. Yang C, Ji S, Li Y, Fu L, Jiang T, Meng F. β-Catenin promotes cell proliferation, migration, and invasion but induces apoptosis in renal cell carcinoma. OncoTargets and Therapy. 2017;Volume 10:711-724.

102. Williams G, Stoeber K. The cell cycle and cancer. The Journal of Pathology. 2011;226(2):352-364.

103. Casimiro M, Crosariol M, Loro E, Li Z, Pestell R. Cyclins and Cell Cycle Control in Cancer and Disease. Genes & Cancer. 2012;3(11-12):649-657.

104. Schafer K. The Cell Cycle: A review. Veterinary Pathology. 1998;35:461-478..

105. Icard P, Fournel L, Wu Z, Alifano M, Lincet H. Interconnection between Metabolism and Cell Cycle in Cancer. Trends in Biochemical Sciences. 2019;44(6):490-501.

106. Kajstura M, Halicka H, Pryjma J, Darzynkiewicz Z. Discontinuous fragmentation of nuclear DNA during apoptosis revealed by discrete "sub-G1" peaks on DNA content histograms. Cytometry Part A. 2007;71A(3):125-131.

107. Buffalo C, Iwamoto Y, Hurley J, Ren X. How HIV Nef Proteins Hijack Membrane Traffic To Promote Infection. Journal of Virology. 2019;93(24).

108. Noy A. Controversies in the treatment of Burkitt lymphoma in AIDS. Current Opinion in Oncology. 2010;22(5):443-448.

109. Lenz G, Salles G. Aggressive Lymphomas. Switzerland (CH): The Springer Nature Switzerland AG; 2019.

110. Rios L. Understanding the molecular pathogenesis of HIV-associated Burkitt Lymphoma – the impact of HIV-1 protein Tat on lymphoma driver genes [Ph.D]. University of Cape Town; 2021.

111. Wolf D, Witte V, Laffert B, Blume K, Stromer E, Trapp S et al. HIV-1 Nef associated PAK and PI3-Kinases stimulate Akt-independent Bad-phosphorylation to induce anti-apoptotic signals. Nature Medicine. 2001;7(11):1217-1224.

112. Said H. Physiology of the Gastrointestinal Tract. 6th ed. Academic Press; 2018.

113. Stoddart M. Mammalian Cell Viability. Totowa, NJ: Springer Science+Business Media, LLC; 2011.

114. Zhao R, Liang D, Li G, Larrimore C, Mirkin B. Anti-Cancer Effect of HIV-1 Viral Protein R on Doxorubicin Resistant Neuroblastoma. PLoS ONE. 2010;5(7):e11466.

115. Lin P, Dickason T, Fayad L, Lennon P, Hu P, Garcia M et al. Prognostic value of MYC rearrangement in cases of B-cell lymphoma, unclassifiable, with features intermediate between diffuse large B-cell lymphoma and Burkitt lymphoma. Cancer. 2011;118(6):1566-1573.

116. Cao E, Chen Y, Cui Z, Foster P. Effect of freezing and thawing rates on denaturation of proteins in aqueous solutions. Biotechnology and Bioengineering. 2003;82(6):684-690.

117. Thorat A, Suryanarayanan R. Characterization of Phosphate Buffered Saline (PBS) in Frozen State and after Freeze-Drying. Pharmaceutical Research. 2019;36(7).

118. Fujii Y, Otake K, Tashiro M, Adachi A. Soluble Nef antigen of HIV-1 is cytotoxic for human CD4+ T cells. FEBS Letters. 1996;393(1):93-96.

119. Fackler O, Kienzle N, Kremmer E, Boese A, Schramm B, Klimkait T et al. Association of Human Immunodeficiency Virus Nef Protein with Actin is Myristoylation Dependent and Influences its Subcellular Localization. European Journal of Biochemistry. 1997;247(3):843-851.

120. Rulifson I, Karnik S, Heiser P, ten Berge D, Chen H, Gu X et al. Wnt signaling regulates pancreatic beta cell proliferation. Proceedings of the National Academy of Sciences. 2007;104(15):6247-6252.

121. Zhao C, Gao J, Li S, Liu Q, Hou X, Liu S et al. Cyclin G2 Suppresses Glomerulosclerosis by Regulating Canonical Wnt Signalling. BioMed Research International. 2018;2018:1-8.

122. Hassanian S, Ardeshirylajimi A, Dinarvand P, Rezaie A. Inorganic polyphosphate promotes cyclin D1 synthesis through activation of mTOR/Wnt/β-catenin signaling in endothelial cells. Journal of Thrombosis and Haemostasis. 2016;14(11):2261-2273.

123. Atallah-Yunes S, Murphy D, Noy A. HIV-associated Burkitt lymphoma. The Lancet Haematology. 2020;7(8):e594-e600.

124. Vishnu P, Aboulafia D. AIDS-Related Non-Hodgkin's Lymphoma in the Era of Highly Active Antiretroviral Therapy. Advances in Hematology. 2012;2012:1-9.

125. Han X, Jemal A, Hulland E, Simard E, Nastoupil L, Ward E et al. HIV Infection and Survival of Lymphoma Patients in the Era of Highly Active Antiretroviral Therapy. Cancer Epidemiology Biomarkers & Prevention. 2016;26(3):303-311.

Appendices:

Appendix A: Recipes and Reagents

Tissue culture

Complete growth media for Ramos and BL-41 cell lines

In a 50 ml Falcon tube:
10% FBS – 5 ml
1% Penicillin/Streptomycin - 0.5 ml
Fill up to 50 ml with RPMI media and mix well
Store at 4°C

Cryo-media for Ramos and BL-41 cell lines

For 5 ml, combine 10% DMSO (500 µl) and 10% FBS (500 µl) in RPMI media (as needed for immediate use)
Place on ice in fume hood until use

Low serum media for pre-treatment (RPMI)

Add 0.1 ml (0.5%) of FBS and 0.2ml (1%) of P/S in a 50 ml Falcon tube
Fill up to 20 ml with RPMI media
Mix well before using for plating cells

Trypsin-EDTA

Dissolve 8 g NaCl, 1.26 g Na2HPO4, 0.2 g KCl, 0.2 g KH2PO4, 0.5 g Trypsin (Sigma) and 0.5 g EDTA in 800 mL dH2O
Adjust pH 7.4
Filter sterilise using 0.2 µm filter
Aliquot into 250 ml bottles and autoclave
Store at 4 ºC.

Complete growth media for HT1080 cell line

In a 50 ml Falcon tube:

10% FBS – 5 ml
1% Penicillin/Streptomycin - 0.5 ml
Fill up to 50 ml with DMEM media and mix well
Store at 4°C

Cryo-media for HT1080 cell line

For 5 ml, combine 10% DMSO (500 µl) and 10% FBS (500 µl) in DMEM media (as needed for immediate use)
Place on ice in fume hood until use

Low serum media for pre-treatment (DMEM)

Add 0.1 ml (0.5%) of FBS and 0.2ml (1%) of P/S in a 50 ml Falcon tube
Fill up to 20 ml with DMEM media
Mix well before using for plating cells

2X Boiling Blue (10 ml)

For 10 ml, combine 1,25 ml of Tris-HCL (pH-6,8); 4 ml 10% SDS; 1 ml β-mercaptoethanol; 2 ml Glycerol; 1,75 ml of deionised water and a pinch of Bromophenol Blue (at room temperature)
Mix well, aliquot and store at -20°C

10 X Phosphate-Buffered Saline (PBS)

Dissolve 1 tablet in 100 ml of deionised water per manufacturer's instructions
Autoclave and store at 4°C

1 X PBS

Add 100 ml of 10X PBS to 900 ml of deionised water
Autoclaved or filter sterilize if necessary
Store at 4°C

Mycoplasma Testing

Antibiotic-free media for mycoplasma testing

10% FBS in RPMI media (make fresh for immediate use, as needed)

Fixative

Mix glacial acetic acid and methanol in a ratio of 1:3 in a 50 ml Falcon tube
Cover the tube with foil and store at 4°C

Mounting Fluid

Combine 22.2 ml 0.1 M citric acid; 27.8 ml 0.2 M Na_2 HPO4.2H_2O and 50 ml glycerol
Adjust to pH 5.5
Aliquot and store at 4°C

Annexin V/7AAD Analysis

1X Annexin Binding Buffer (15 ml)

Add 1,5 ml of 10X Annexin Binding buffer to 13,5 ml of deionised water
Use immediately or store covered in foil at 4°C.

Cell Cycle Profiling

RNAse A solution (1,5 ml)

Based on the cell count which was 30×10^4 cells/ml in 10 mls, thus the volume of RNAse A solution required is 300 µl.
Add 7,5 µl of RNAse A (10 mg/ml) to 1,5 ml of 1X PBS
Use immediately

Propidium Iodide staining solution (11 ml)

Mix 110 µl PI stock (1 mg/ml) with 11 µl (0,1%) Triton X-100 to 15 ml tubes.
Top up till 11 ml with 1X PBS
Cover tube with foil and keep on ice till use

Protein Extraction

RIPA buffer

Dissolve 0.5 g (1%) deoxycholate powder in 40 ml deionized water
Combine with the following: 1.5 ml 5M NaCl (150 mM); 0.5 ml Triton X100 (1%); 0.25 ml 20% SDS (0.1%) and 0.5 ml 1M Tris **(**pH 7.5) (10 mM)
Top up to 50 ml with deionized water
Store at 4°C

7X protease inhibitor

Dissolve 1 protease inhibitor tablet in 2.5 ml 1X PBS
Store at -20°C

RIPA solution

Mix 423 µl RIPA buffer and 71 µl 7X protease inhibitor
Store on ice until use

Western blot analysis

SDS-PAGE reagents:

30% acryl-bisacrilamide

29 g acrylamide
1 g N.N'-methylenbisacrylamide
Dissolve in 60 ml deionised water
Heat the solution to 37°C
Adjust volume 100 ml and cover with foil to protect from light
Store at 4°C

1.5M Tris buffer (pH 6.8)

Dissolve 60.5 g Tris in 300 ml deionised water
Adjust pH to 6.8 with HCl
Fill up to 500 ml with deionised water

Store at 4°C

1.5M Tris buffer (pH 8.8)

Dissolve 60.5 g Tris in 300 ml deionised water
Adjust pH to 8.8 with HCl
Fill up to 500 ml with deionised water
Store at 4°C

10% Sodium dodecyl (SDS)

Dissolve 5 g SDS in 40 ml deionised water
Fill up to 50 ml with deionised water
Store at room temperature

0.1% SDS

Dissolve 0.05 g SDS in 40 ml deionised water
Adjust volume to 50 ml with deionised water
Store at room temperature

10% Ammonium persulfate (APS)

Dissolve 0.1 g APS in 1 ml deionised water
Cover tube with foil and store at 4°C

15% resolving gel for SDS-PAGE (7,5 ml)

1.65 ml deionised water
3.75 ml 30% acryl-bisacrylamide
1.95 ml 1.5M Tris (pH 8.8)
0.075 ml 10% SDS
0.075 ml 10% APS
0.005 ml tetramethylethylenediamine (TEMED) (under the fume hood)
Mix and pour between the glass plates in gel casting apparatus using a 10 ml glass beaker
Add 2 ml 0.1% SDS on top to even the gel out and allow to set.
Pour out the SDS after the gel has set.

5% Stacking gel for SDS-PAGE (3 ml)

2.1 ml deionised water
0.5 ml 30% acryl-bisacrylamide
0.38 ml 1.5M Tris (pH 6.8)
0.03 ml 10% SDS
0.03 ml 10% APS
0.005 ml tetramethylethylenediamine (TEMED) (under the fume hood)
Mix and pour on top of the resolving gel between the glass plates
Add comb and allow to set

5X SDS loading dye

0.04 g Bromophenol blue (0.04%)
10 g SDS (10%)
Dissolved in 52.5 ml deionised water
12.5 ml 2M Tris (pH 6.8)
30 ml 100% glycerol
5 ml β-mercaptoethanol
Mix, aliquot and store at room temperature

10X SDS-PAGE running buffer

10 g SDS
30.3 g Tris
144.1 g glycine
Dissolve in 800 ml deionised water
Adjust to 1 litre with deionised water and store at room temperature

1X SDS-PAGE running buffer

100 ml of 10X SDS-PAGE running buffer stock
900 ml deionised water
Mix and store at room temperature

Coomassie Blue Staining solution (100 ml)
Dissolve 0.25 g Coomassie Brilliant Blue R-250 in a mixture of 45 ml methanol, 10 ml acetic acid, and 40 ml deionised water.
Adjust volume to 100 ml with deionised water.

Store at room temperature.

Destaining solution (1 litre)

Mix 450 ml methanol, 100 ml acetic acid, and 400 ml deionised water.

Adjust volume to 1 litre with deionised water.

Store at room temperature.

10X SDS-PAGE transfer buffer

38 g Tris

144 g glycine

Dissolve in 800 ml deionised water

Adjust volume to 1 litre with deionised water and store at room temperature

1X SDS-PAGE transfer buffer

100 ml 10X SDS-PAGE transfer buffer stock

700 ml deionised water

200 ml Isopropanol

Make in advance and store at 4°C

Protein detection and washing:

0.1% (w/v) Ponceau S staining solution, in 5% (v/v) acetic acid

0.05 g Ponceau S

2.5 ml Acetic acid (5%)

Dissolve and adjust volume to 50 ml with deionised water

Cover with foil to protect from light and store at room temperature

1X PBS/0.1% Tween (PBS-Tween)

1 ml Tween-20 to 1 litre of 1X PBS

Add magnetic stirrer bar and place on magnetic stirrer

Mix well, remove stirrer bar and store at 4°C

Blocking buffer

41.7 ml fat-free milk (5%)

58.3 ml PBS-Tween
Mix and store at 4°C

Stripping buffer

0.69 ml 100 Mm β-mercaptoethanol
10 ml 2% SDS
6.25 ml 62.5 mM Tris (pH 6.7)
Adjust to 100 ml with deionised water
Store at room temperature

Appendix B: Additional Data

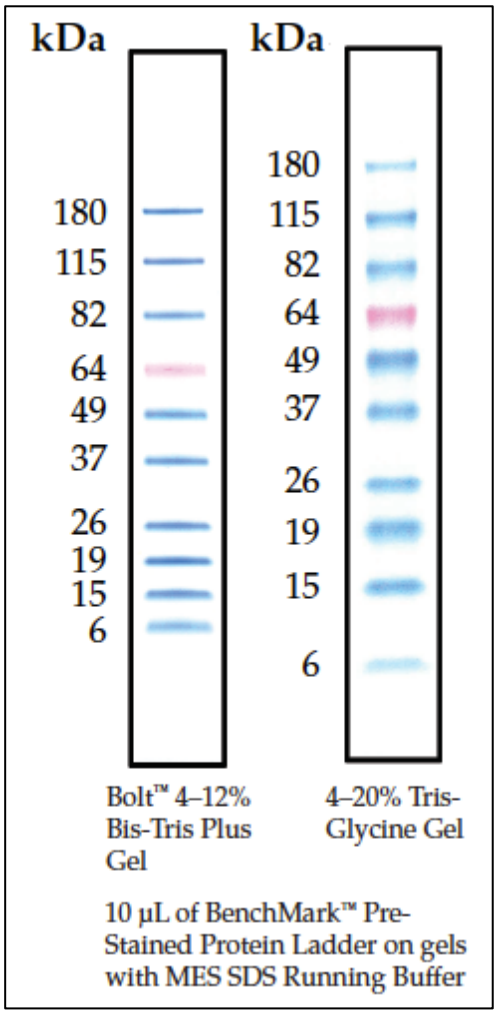

Figure B1: BenchMark™ Pre-Stained Protein Ladder

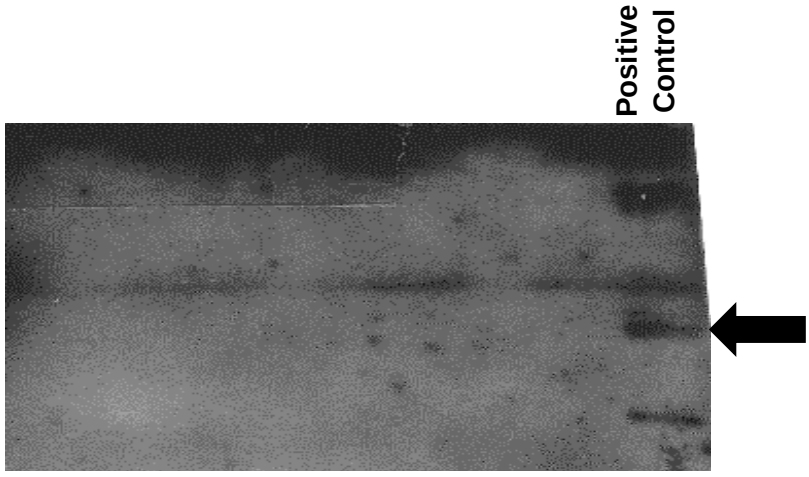

Figure B2: Western blotting analysis of HT1080 cells transfected with Nef-expressing mammalian expression construct (Positive Control). The black arrow indicates the Nef protein